Case Report

Not peer-reviewed version

Total Reversal of ALS Confirmed by EMG Normalization and Neuromuscular–Molecular Evidence Achieved Through Computerized Brain-Guided Reengineering of the 1927 Nobel Prize Fever Therapy: A Video-Documented Case Report

M Marc Abreu *, Mohammad Hosseini Farid, David G Silverman *

Posted Date: 4 September 2025

doi: 10.20944/preprints202509.0342.v1

Keywords: amyotrophic lateral sclerosis; ALS treatment; ALS; computerized brain-guided intelligent thermofebrile therapy; heat shock protein; brain-eyelid thermoregulatory tunnel; fever therapy; neurodegeneration reversal; Nobel prize–recognized malarial fever therapy

 doi:10.20944/preprints202509.0342.v1

Case Report

Total Reversal of ALS Confirmed by EMG Normalization and Neuromuscular–Molecular Evidence Achieved Through Computerized Brain-Guided Reengineering of the 1927 Nobel Prize Fever Therapy: A Video-Documented Case Report

M Marc Abreu [1,2,*], Mohammad Hosseini-Farid [3] and David G Silverman [4,*]

[1] Clinical Sciences Division, BTT Medical Institute, Aventura, FL, USA
[2] Department of Biomedical Engineering and Medical Physics, BTT Medical Institute, Aventura, FL, USA
[3] College of Computing and Engineering, Nova Southeastern University, Fort Lauderdale, FL, USA
[4] Department of Anesthesiology, Yale University School of Medicine, New Haven, CT, USA
* Correspondence: mabreu@bttmedicalinstitute.com (M.M.A.); david.silverman@yale.edu (D.G.S.)

Abstract

Background: Neurological disorders are the leading cause of disability, affecting over three billion people. Amyotrophic lateral sclerosis (ALS) is among the most feared and uniformly fatal neurodegenerative diseases, with no therapy capable of restoring function. **Methods:** We report the first application of therapeutic fever to ALS using Computerized Brain-Guided Intelligent Thermofebrile Therapy (CBIT²). This fully noninvasive treatment, delivered through FDA-approved computerized platform, digitally reengineers the 1927 Nobel Prize–recognized malarial fever therapy into a modern treatment guided by the Brain–Eyelid Thermoregulatory Tunnel. CBIT² induces therapeutic fever through synchronized hypothalamic feedback, activating heat shock proteins to restore proteostasis and neuronal function. **Case Presentation:** A 56-year-old woman with rapidly progressive ALS was diagnosed at the Mayo Clinic, based on electromyography showing denervation and fasciculations corroborated by neurological and MRI findings; and patient was informed of an expected 3–5-year survival. Northwestern University independently confirmed the diagnosis and maintained her on FDA-approved ALS drugs (riluzole and edaravone). Her condition worsened and she underwent CBIT², resulting in: (i) electrophysiological reversal with disappearance of denervation and fasciculations; (ii) biomarker correction, including reductions in neurofilament and homocysteine, besides IL-10 normalization (previously linked to mortality) alongside robust HSP70 induction; (iii) restoration of gait, swallowing, respiration, speech, and cognition; and (iv) return to complex motor tasks, including golf and pickleball. **Discussion/Conclusions:** This case provides the first documented evidence that ALS can be reversed through digitally reengineered fever therapy aligned with thermoregulation. Beyond ALS, shared protein-misfolding pathology suggests CBIT² may extend to Alzheimer's, Parkinson's, and related disorders. By modernizing a Nobel Prize–recognized therapeutic principle with digital precision, CBIT² establishes a framework for large-scale clinical trials. Just as fever therapy a century ago restored lost brain function in dementia paralytica and earned the 1927 Nobel Prize, CBIT² now safely harnesses the therapeutic power of fever through brain-guided modulation. Amid a global brain health crisis, where neurological disorders affect more than three billion people, fever-based therapies may provide a path to preserve thought, memory, movement, and independence for over one third of humanity.

 doi:10.20944/preprints202509.0342.v1

Keywords: amyotrophic lateral sclerosis; ALS treatment; ALS; computerized brain-guided intelligent thermofebrile therapy; heat shock protein; brain-eyelid thermoregulatory tunnel; fever therapy; neurodegeneration reversal; Nobel prize–recognized malarial fever therapy

1. Introduction

"*We have an urgent global brain health crisis… No country has a handle on this escalating challenge*" [1]. With those stark words, the June 2025 G7 Summit of the world's leading economies presented the sobering reality that even the most technologically advanced nations, equipped with cutting-edge science, medical technology, advanced pharmaceuticals, and artificial intelligence, remain powerless in the face of an accelerating neurological epidemic. No country, regardless of wealth or scientific expertise, has succeeded in containing this brain health crisis [1]. The alarming G7 declaration echoed the World Health Organization (WHO) warning in 2024 that neurological disorders now affect more than one in three people, over three billion individuals, and have become the leading cause of disability worldwide [2], reflecting the lack of treatments capable of restoring lost neurological function.

If left unaddressed, the trajectory is unmistakable. In the absence of therapies capable of reversing disease, neurological diseases will not only disable but ultimately kill, reducing human potential on an unprecedented scale. This staggering loss of human life is no longer theoretical as the WHO has issued a grave warning that neurological disorders are projected to become the second leading cause of death worldwide [3], confirming that today's crisis of neurological disability is rapidly escalating into a global mass mortality event with catastrophic humanitarian and socioeconomic consequences.

Among the most feared and devastating manifestations of neurological diseases stands Amyotrophic Lateral Sclerosis (ALS), a progressive fatal neurodegenerative disorder characterized by paralysis [4,5], and often dementia [6,7], that strikes without warning and strips away the most basic human abilities such as moving, speaking, swallowing and breathing. ALS gained widespread recognition following the death of New York Yankees Hall of Fame baseball star Lou Gehrig at age 37, demonstrating that neither youth, peak physical fitness, nor elite athletic performance confers protection against the disease's indiscriminate nature [8,9].

Long considered untreatable, ALS follows a brutal course toward paralysis, respiratory failure, and death, devastating lives and revealing the failure of global scientific research to develop a disease reversal treatment for brain disorders. Confronting this challenge demands not only new treatments, but an entirely new way of thinking. And yet, the most transformative idea may not be new at all, but one discovered a century ago in the form of malarial fever therapy effectively restoring neurological function in dementia paralytica, which was honored with the Nobel Prize in Medicine [10–18], suggesting that the path to solving the global brain health crisis was not only foreseen through Nobel wisdom but scientifically validated; awaiting not invention, but rediscovery, and rising again 100 years later not as memory, but as method.

The convergence of a Nobel Prize–recognized treatment and advanced digital engineering has unlocked a novel approach, reviving a long-overlooked path that may change the course of the global brain health crisis with a scientifically grounded method that herein has achieved neurological, molecular, and electrophysiological reversal of ALS, opening the path to treating a wide range of neurodegenerative diseases previously deemed irreversible. This path for effectively treating neurological disorders was made possible by the approval of a computerized platform by the U.S. Food and Drug Administration (FDA), publicly announced by ASUS Computer Company [19], which enabled the development of Computerized Brain-guided Intelligent Thermofebrile Therapy (CBIT²) that digitally reengineers the 1927 Nobel Prize–winning malarial fever therapy that once achieved the unthinkable by reversing paralysis and dementia in patients neurologically condemned to death [10–18].

 doi:10.20944/preprints202509.0342.v1

To counteract ongoing neuronal loss and progressive incapacitation in a 56-year-old patient with rapidly advancing ALS, we use CBIT², a digitally controlled, fully noninvasive, intelligent, noninfectious, fever-based therapy with no adverse effects designed to regulate the brain thermoregulatory response and cerebral molecular heat shock repair systems. Using digital precision and real-time thermoregulatory feedback, CBIT² was employed to induce heat shock protein (HSP) in the brain, specifically targeting motor neurons, aiming to counteract a biomarker-confirmed trajectory of rapid disease progression and impending demise in this ALS patient while reversing neurodegeneration and overcoming the well-documented limitations of existing ALS therapies. Current ALS treatments offer only marginal delays in functional decline and brief extensions of life by about two to three months, while failing to arrest or reverse neuronal loss, progressive incapacitation, and death [20–23].

This report emerges in the context of this mounting global neurological crisis [1,2]. Paradoxically, it is ALS, long considered an intractable and fatal neurodegenerative disorder, that may offer a path towards a solution to the global neurological emergency. Given ALS's uniquely high threshold for inducing HSPs in motor neurons [24], the remarkable combination of neurological, molecular, and electrophysiological reversal observed in this ALS patient suggests broader therapeutic potential that extends well beyond a single neurological disease as neurodegeneration share common features of progressive neuronal loss driven by pathological protein aggregation [25,26]. Among these disorders, ALS may serve as the ultimate proving ground; if reversal is achievable in this most treatment-resistant condition [27], then applying similar therapeutic approach to less refractory neurological diseases as Alzheimer's disease, Parkinson's disease, ataxia and related pathologies may not only be plausible, but imminently within reach. Thus, ALS shifts from a symbol of irreversible decline and death to a therapeutic gateway, offering a path forward in the broader fight against neurological disorders that increasingly disrupt global health and economic stability.

Although this case moves from infection to invention, it is not merely a testament to technological progress, but in fact it reclaims a therapeutic truth first revealed through Nobel-winning malarial fever, which is the only treatment in history to cure dementia paralytica and empty the asylums once filled with the terminally afflicted with this fatal neuropsychiatric disorder [10–18]. This report opens the door ethically, scientifically, and humanely to a complementary path that includes infection as intervention, fever as medicine, especially if it offers a means to restore proteostasis and prevent the collapse of neurological health for billions around the world.

In this context, effective HSP induction shown herein after computerized fever-based therapy, led to the neurological, molecular, and electrophysiological reversal of ALS, providing direct evidence that correcting misfolded protein dysfunction can reverse disease. This therapeutic rational becomes even more compelling when considering that the molecular basis of neurodegeneration is impaired HSP function, leading to misfolded protein accumulation and neuronal damage, which leads to disease progression [28–30]. Furthermore, increased HSP70 reduces protein aggregation and supports motor neuron survival [31,32], while HSP27 and HSP90 influence neuroprotection or disease progression based on their expression levels [33,34]. Moreover, HSP-based pharmacological interventions have been considered for Alzheimer's, Parkinson's, Huntington's, and ALS [35–39], aiming to correct chaperone dysfunction and restore proteostasis, and potentially slow ALS progression [40]. Recent attempts to upregulate HSPs using agents like arimoclomol showed increased HSP expression in animal models but failed to improve clinical outcomes and raised safety concerns at higher doses [20]. Nonetheless, HSP activation may hold therapeutic and neuroprotective potential, as detailed in a recent review by Smadja and Abreu [26] and emerging evidence suggests that heat acclimation and passive heat therapy may induce HSP expression and reduce the risk of Alzheimer's and Parkinson's disease [41]. However, although the relationship between hyperthermia and HSP activation is established [26], thermal treatment has never been applied to ALS, and its use to counter, much less reverse, the associated paralysis and cognitive decline, has not yet been explored.

 doi:10.20944/preprints202509.0342.v1

We herein demonstrate the therapeutic effects of CBIT² in ALS, with evidence of disease reversal and restoration of motor neuron function, validated by objective neuromuscular assessments, normalization of molecular biomarkers, and upregulation of heat shock protein expression. Strikingly, electrophysiological studies revealed the complete disappearance of denervation, the defining hallmark of motor neuron death in ALS, along with the resolution of fasciculations, both clearly present before our treatment but absent following CBIT². This electrophysiological reversal of ALS following CBIT² was independently validated at two of the foremost university-based neurology centers in the United States (for electromyography report see Appendix A), providing rigorous, objective confirmation of motor neuron restoration, offering objective evidence for the reversal of neurodegeneration in a condition long considered irreversible. What was once deemed impossible in ALS occurred following CBIT², as electromyography demonstrated the complete disappearance of denervation, providing objective electrophysiological evidence for the absence of motor neuron degeneration.

As alluded to above, the protocol used by CBIT² is derived from a landmark moment in medical history, when Austrian psychiatrist Dr. Julius Wagner-Jauregg was awarded the Nobel Prize in Medicine for his pioneering use of high fever induced by malarial infection to treat dementia paralytica, a disorder marked by fatal paralysis and profound cognitive decline representing the terminal stage of neurosyphilis [10–18]. As highlighted in a review, the impact of malarial fever therapy was dramatic: "*Death, in most cases, was welcomed as the final respite from the horrifying symptoms of neurosyphilis... malarial treatment played a role in the emptying of the asylums and provided a viable alternative for a previously hopeless disease*" [11].

Dr. Wagner-Jauregg initially used erysipelas and tuberculin to induce therapeutic fever with limited success and severe side effects. His breakthrough came with the use of malarial fever, which produced remarkable neurological recovery in patients with dementia paralytica, ultimately establishing the treatment as a curative therapy for otherwise intractable neuropsychiatric symptoms Prize [10–18]. At the time, the therapeutic benefit was largely attributed to fever's presumed ability to eliminate *Treponema pallidum*, the pathogen causing syphilis, rather than to any reversal of brain disease, which is the innovative therapeutic paradigm newly proposed here. As further evidence supporting bacterial eradication as the therapeutic rationale a century ago, some physicians advocated initiating malarial fever therapy immediately following a positive Wassermann test, even before the onset of dementia paralytica, as a preventive intervention against neurosyphilis [11]. Despite its remarkable success in Europe and across the world, malarial fever therapy faded into obscurity with the advent of antibiotics (to prevent progression of syphilis to its tertiary stage) and ethical concerns about potential serious risks due to malarial infection including migration of the parasite to the brain causing cerebral malaria, which is commonly fatal [10–18].

Nearly a century later, M. Marc Abreu, M.D. (primary author) critically reexamined Wagner-Jauregg's original data and uncovered a striking and long-overlooked possibility that malarial fever therapy may have reversed not only the underlying syphilitic infection but also the structural brain injury that persisted even after microbial eradication. Abreu observed that the progressive paralysis seen in dementia paralytica closely resembles the motor deterioration characteristic of ALS. Remarkably, these two seemingly unrelated diseases are united by a shared molecular signature in which both are driven by the pathological accumulation of misfolded TDP-43, the defining biomarker of ALS [42], which astonishingly also aggregates in neurosyphilis [43]. This unexpected molecular signature spanning a century offers compelling scientific support that the curative principles behind the 1927 Nobel Prize therapy may hold similarly curative promise for ALS today.

Molecular evidence implicating misfolded TDP-43 as a central driver of neurodegeneration, together with clinical reports showing that malarial fever therapy from tertian malaria, with fevers reaching up to 41.5 °C, reversed neuronal damage and enabled full neurological recovery with reintegration into daily life [10–18], demonstrated that neurodegeneration can, in fact, be reversed. Multiple reports from around the world describe patients once bound by paralysis and seemingly condemned to death, who, after undergoing malarial fever therapy, regained speech, recovered

 doi:10.20944/preprints202509.0342.v1

movement, returned to work, and experienced what can only be described as a neurological rebirth [10–18]. Building on these extraordinary outcomes achieved by Nobel laureate Dr. Wagner-Jauregg, and recognizing the need for a safe, effective, and noninfectious alternative, Abreu developed a computerized, digitally controlled, intelligent, hypothalamic-guided platform designed to replicate the high fever patterns of malarial infection to target the core molecular dysfunction of misfolded protein, offering a novel pathway to restore what has long been considered irreversible neurodegeneration.

The safe titration of brain temperature and the generation of computerized cyclical thermal patterns under hypothalamic control were made possible by Abreu's discovery at Yale University School of Medicine of a biological thermal waveguide between the brain and eyelid, known as the Brain-Eyelid Thermoregulatory Tunnel (BTT), initially described as the brain temperature tunnel [44–46]. The discovery of the BTT led to the development of a computerized platform and sensor system approved by the U.S. FDA which laid the technological foundation for CBIT² which includes noninvasive measurement of brain temperature and real-time, brain-guided, intelligent induction of the heat shock response (Abreu BTT 700 Computer System, Heat Shock Induction 700 Module, Brain Tunnelgenix Technologies Corp., Aventura, Florida).

Agreement with body core temperature, except for specificity to the brain during brain–core discordance, was demonstrated in Yale-led studies by Abreu and Silverman (co-author) in collaboration with other institutions [46] as well as in a multi-institutional study led by Nova Southeastern University, in Florida, which cited the Yale findings in an article assessing the impact of carotid temperature modifications on brain temperature and yawning [47].

Misfolded protein pathology common to both neurosyphilis [43] and ALS [42], together with global clinical evidence of fever-induced neurological recovery [10–18], provided the foundation for transforming a century-old, Nobel-recognized therapy into CBIT² as a computerized, noninvasive, hypothalamic-targeted, AI-enhanced platform that titrates brain temperature to reverse neurodegeneration. Consistent with the rhythmic nature of malarial fever therapy, Abreu hypothesized that such patterned thermal input triggers repeated activation of the heat shock response, upregulating HSPs that support neuronal protection and recovery [28–33,40], and further proposed that cerebral HSP induction may respond more effectively to dynamic thermal profiles across distinct brain regions [48].

Noninvasive brain temperature and thermodynamics monitoring were critical to both the safety and efficacy of CBIT², allowing real-time assessment of cerebral thermodynamics, precise titration of the thermofebrile response based on hypothalamic signals, prevention of hyperthermic brain injury, and direct delivery of therapeutic heat to the brain. These advantages are especially critical in ALS, where motor neurons require higher thermal threshold to induce heat shock response, including robust expression of HSP70 [24]. Guided by the BTT, CBIT² delivers precise, cyclical high-heat exposure to activate HSPs within thermally resistant motor neurons [24], replicating the therapeutic mechanism of malarial fever in a computerized, infection-free platform.

Guided by continuous, minute-by-minute thermal measurements to guide real-time adjustments, the protocol ensures precise brain modulation and patient safety, bringing to life Lord Kelvin's timeless words *"You cannot manage what you cannot measure"* [49]. We further apply Kelvin's tenet to this case through quantitative documentation of clinical improvement, including enhanced motor function, reductions in pathological serum biomarkers, measurable increases in HSP expression, and numerical evidence of electrophysiological restoration, in addition to written reports from the patient and her physical therapist. Complementing this approach, a defining and unique strength of this case report is the integration of pre- and post-treatment video documentation, which provided direct visual validation of neurological recovery, corroborating findings from electromyography (EMG) and blood biomarker normalization. This convergence of objective clinical, molecular, and electrophysiological data with real-time video documentation not only confirmed individual patient outcomes but also reinforced the broader scientific rationale underlying CBIT², based on the long-overlooked therapeutic principles of malarial fever therapy.

 doi:10.20944/preprints202509.0342.v1

The forgotten, more aptly both unrecognized and unappreciated, link between the 1927 Nobel Prize discovery and the treatment of neurodegenerative disease laid the foundation for a safe, infection-free, computer-controlled hub of therapeutic intelligence, capable of dynamically modulating and personalizing therapy in real time. By digitally reengineering the century-old, Nobel-recognized fever rhythms that once reversed disease and restored function in patients with paralysis and dementia, CBIT² delivers precise, brain-guided replication of the cyclical thermal dynamics of malarial infection to treat neurodegeneration. CBIT² seeks to reverse what has long been considered irreversible, now demonstrated by EMG, where denervation once signaled motor neuron death and renewed electrical activity now indicates restored neuronal function following brain-guided programmed fever therapy.

Thus, against this escalating global brain health crisis highlighted by the G7 Summit and WHO [1,2], reawakened Nobel wisdom, without which the computerized fever therapy shown here could never have been conceived, now opens a therapeutic path where none was thought to exist, offering what may represent a novel intervention to defend the human brain in the age of intelligent machines.

From the 1927 Nobel Prize–recognized malarial fever therapy, once used to reverse paralysis and dementia in neurosyphilis, emerges a modern reengineering grounded in the understanding of misfolded protein pathology and the molecular biology of the heat shock response. Through AI-enhanced brain thermodynamics, the rhythmic thermal patterns once generated unpredictably by infection can now be delivered with precision, safety, and hypothalamic targeting, transforming an abandoned historical intervention into a controllable, noninvasive neurotherapeutic platform.

On this basis, the present case report, which documents neurological, molecular, and electrophysiological reversal of ALS following CBIT², provides clinical evidence that the core therapeutic mechanism behind malarial fever therapy is plausibly the induction of the heat shock response, a process that can now be noninvasively reengineered, precisely targeted, and dynamically controlled through AI-enhanced brain thermodynamics. Enabled by U.S. FDA approval of our computerized platform, CBIT² builds on this technological foundation to transform the century-old, Nobel-recognized fever therapy into a modern, infection-free, brain-guided intervention capable of precise thermoregulatory targeting. Through the convergence of Nobel-recognized therapy and advanced digital engineering, a therapeutic approach now emerges to confront what was once considered untreatable, offering a potential pathway to alter the course of neurological decline and change the trajectory of brain disability and death on a global scale.

Case Report

A 56-year-old female patient with a confirmed diagnosis of ALS was referred to the BTT Medical Institute in Florida following a progressive and marked decline in motor function. On October 25, 2024, she had been diagnosed with ALS at the Mayo Clinic in Rochester, Minnesota, which is recognized as the leading neurology hospital in the United States [50].

Her past medical history was otherwise unremarkable, aside from a cervical fusion at the C3–C5 vertebrae without residual sequelae. Family history was negative for dementia, neurological disorders, or muscle disease. She denied smoking or recreational drug use and reported consuming socially approximately one alcoholic drink per week. In May 2019, she developed mild stiffness and spasticity in both legs following a fall, which led to recurrent falls. Initially suspected of having Stiff Person Syndrome, she was treated with intravenous immunoglobulin (IVIg) and diazepam, but her symptoms failed to improve and progressively worsened. In September 2023, she developed dysphagia and dysarthria worsening in the evenings despite a reduction in her diazepam dosage.

The cornerstone for the diagnosis of ALS is electromyography (EMG) showing denervation. EMG was performed at the Mayo Clinic on October 25th, 2024 and demonstrated active denervation and reinnervation in the lumbosacral segment with chronic denervation in the right hand in addition to fasciculations demonstrating lower motor neuron changes. The Mayo Clinic report further documented progressive weakness of hand grip, more pronounced on the right side, along with progressive spasticity of the lower extremities and worsening gait, now requiring a walker after

 doi:10.20944/preprints202509.0342.v1

previously using a cane. The patient also presented with dysarthria, episodes of coughing when drinking liquids, and nasal regurgitation. On examination, gait was markedly spastic; she was unable to walk on heels or toes and could not rise from a chair. Additional findings included a positive Hoffmann sign, weakness of the right arm and hand, and weakness involving the knee, ankle, and toes. Taken together, these findings confirmed combined upper and lower motor neuron involvement, characteristic of ALS. The Mayo Clinic neurologist stressed that "*progressive lower motor neuron denervation is unfortunately inevitable*" and that *"The median patient survival is 3–5 years from symptom onset considering all ALS patients, but some patients have a more rapid or slowly progressive curve."* The patient was enrolled in the ALS Clinic and prescribed FDA–approved drugs for ALS, namely riluzole and edaravone.

MRI demonstrated susceptibility-weighted imaging (SWI) changes in the motor band together with corticospinal tract (CST) hyperintensity on FLAIR (fluid-attenuated inversion recovery) in the pons and cerebellar peduncles. The combined presence of the motor band sign on SWI and corticospinal tract hyperintensity on FLAIR has been reported to carry high specificity for ALS, thereby providing additional radiologic corroboration of the diagnosis of ALS. A series of tests and evaluations were performed to rule out alternative diagnoses, including Lyme serology and a long-chain fatty acid panel, which returned normal, and testing for myasthenia gravis, M protein, creatine kinase (CK), hemoglobin A1c, and thyroid-stimulating hormone (TSH), all of which were negative.

The patient's diagnostic and therapeutic journey spanned two of the most prestigious neurology institutions in the United States. She was initially diagnosed and treated at the Mayo Clinic and later at Northwestern University, a nationally ranked neurology center in Illinois, where she resides. Together, these centers represent the pinnacle of neurological expertise, yet her rapidly declining course underscores the reality that even care delivered at the most elite institutions, by some of the foremost neurologists in the field, remains constrained by the limited efficacy of current ALS therapies. Her neurological function continued to deteriorate despite treatment with two FDA-approved therapies for ALS, which are known to provide only modest clinical benefit. This trajectory highlights not only the limitations of standard pharmacologic options but also the urgent need for alternative therapeutic strategies capable of reversing disease and restoring lost neurological function.

A neurological examination performed at Northwestern on December 4, 2024 documented mixed dysarthria and a spastic gait. Cranial nerve examination revealed a weak cheek puff and slow tongue movement. Motor examination revealed reduced motor strength and spasticity, predominantly in the right leg as well as positive Romberg, Hoffman and Tromner's signs (more pronounced on the right). The patient had limited range of motion, but no bony abnormalities, contractures, malalignment, or tenderness.

The patient learned about brain-guided programmed fever therapy from an acquaintance who had previously been successfully treated at the BTT Medical Institute. A pre-treatment examination performed at the BTT Medical Institute in Florida on January 28, 2025, confirmed findings consistent with prior evaluations at the Mayo Clinic and Northwestern University, detailed here. However, by this time her gait had become irregular, wide-based, and waddling, with severely limited ambulation requiring the use of a walker. Coordination and cerebellar testing revealed an intact finger-to-nose performance without tremors. Her current medications included diazepam 5 mg once daily by mouth, Sertraline 50 mg once daily by mouth, dextromethorphan/quinidine 10 mg twice daily by mouth, riluzole 50 mg twice daily by mouth, and edaravone 5 mL once daily by mouth. Ongoing and supportive management consisted of physical therapy, speech therapy, and symptomatic treatment aimed at managing spasticity, dysarthria, and dysphagia.

We sought to determine whether Computerized Brain-Guided Intelligent Thermofebrile Therapy (CBIT^2), delivered through an FDA-approved computerized platform that includes a Thermofebrile Rhythm Engineering Protocol, could acutely halt, or even reverse, the ongoing neurodegeneration and motor neuron loss due to ALS present in this patient. This application of CBIT^2 in a patient with a neurodegenerative disorder was guided by the hypothesis that it could

 doi:10.20944/preprints202509.0342.v1

reproduce the curative effects once achieved with malarial fever therapy, grounded in the shared pathological hallmark of TDP-43 proteinopathy present in both ALS and dementia paralytica (neurosyphilis), which is the disease effectively treated by Wagner-Jauregg's Nobel Prize–winning discovery.

To rigorously evaluate this potential, a comprehensive battery of assessments was conducted, including quantitative neuromuscular testing tailored to the patient's symptom profile, high-resolution gait and balance analysis, respiratory function testing, oral motor strength evaluation, and upper and lower limb strength measurement. Serial blood biomarkers were monitored to assess disease burden and therapeutic response, including neurofilament light chain (NfL), homocysteine, interleukin-10 (IL-10), and heat shock protein (HSP) expression. Complementing these molecular assessments, electrophysiological studies including pre- and post-treatment EMGs spaced five months apart were conducted by independent university-based services to evaluate changes in motor unit integrity and neuromuscular signaling. The EMG protocol was designed to detect both the silence that accompanies motor neuron death and the reemergence of electrical activity that could signify reinnervation. In this way, the electrophysiological data provided a real-time window into the absence of denervation following CBIT² and neuronal restoration, engraved into the muscles themselves. Together, this multidimensional evaluation including neuromuscular assessment, serial biomarkers, and electrophysiological studies enabled a robust appraisal of both functional and structural recovery as well as molecular response to this novel, noninvasive, computerized intelligent thermofebrile neurotherapeutic intervention.

2. Therapeutic Intervention

2.1. Computerized, Intelligent Thermal Delivery via Radiative–Conductive Integration and Hypothalamic Feedback Modulation

Following a comprehensive explanation of CBIT² including potential risks and benefits, informed consent was obtained. The procedure was conducted in accordance with U.S. FDA regulations, utilizing an FDA-approved computerized platform. The patient received CBIT², a dual-modality therapy that noninvasively delivers therapeutic fever through programmed radiant and conductive thermal delivery to the skin, integrated with hypothalamic neuroregulatory feedback. The intervention was administered through the BTT system using the FDA-approved Abreu-BTT 700 System (Brain Tunnelgenix Technologies Corp, Aventura, Florida, USA), which integrates the BTT sensor assembly, a BTT radiant-heat chamber, and an eyelid-mounted BTT thermal inductor (see schematic Figure 1).

Central to the CBIT² is the Thermofebrile Rhythm Engineering Protocol, which transforms brain temperature from a static measurement into a continuously monitored, dynamic pattern that is algorithmically recognized and modeled on the thermal rhythm of malarial fever, then reinterpreted within a controlled, brain-mediated, noninfectious, and precision-guided algorithm. CBIT² digitally reengineers and intelligently condenses the malaria fever-based therapy first introduced by Wagner-Jauregg in his Nobel Prize–winning treatment of dementia paralytica, preserving its therapeutic objectives and cyclical dynamics while enabling safe, precise, and noninvasive brain-guided therapy.

CBIT² reproduces a three-phase thermofebrile cycle—ramp-up, peak, and resolution—modeled on the cyclical dynamics of Nobel Prize–winning malariotherapy. Traditional Plasmodium vivax-induced febrile paroxysms consist of three distinct stages across 8 to 12 hours: a cold stage lasting 1 to 2 hours, a hot stage of approximately 4 hours with peak temperatures reaching 41.6 °C, and a sweating stage of 2 to 4 hours. These stages correspond directly to the CBIT² phases, now replicated in a noninfectious, algorithmically controlled triphasic structure of natural fever. The CBIT² protocol condenses the entire cycle into a tightly regulated session of approximately 2.5 to 5.0 hours, with duration customized to each patient's thermoregulatory response profile, pre-treatment biomarkers, and individual clinical requirements.

 doi:10.20944/preprints202509.0342.v1

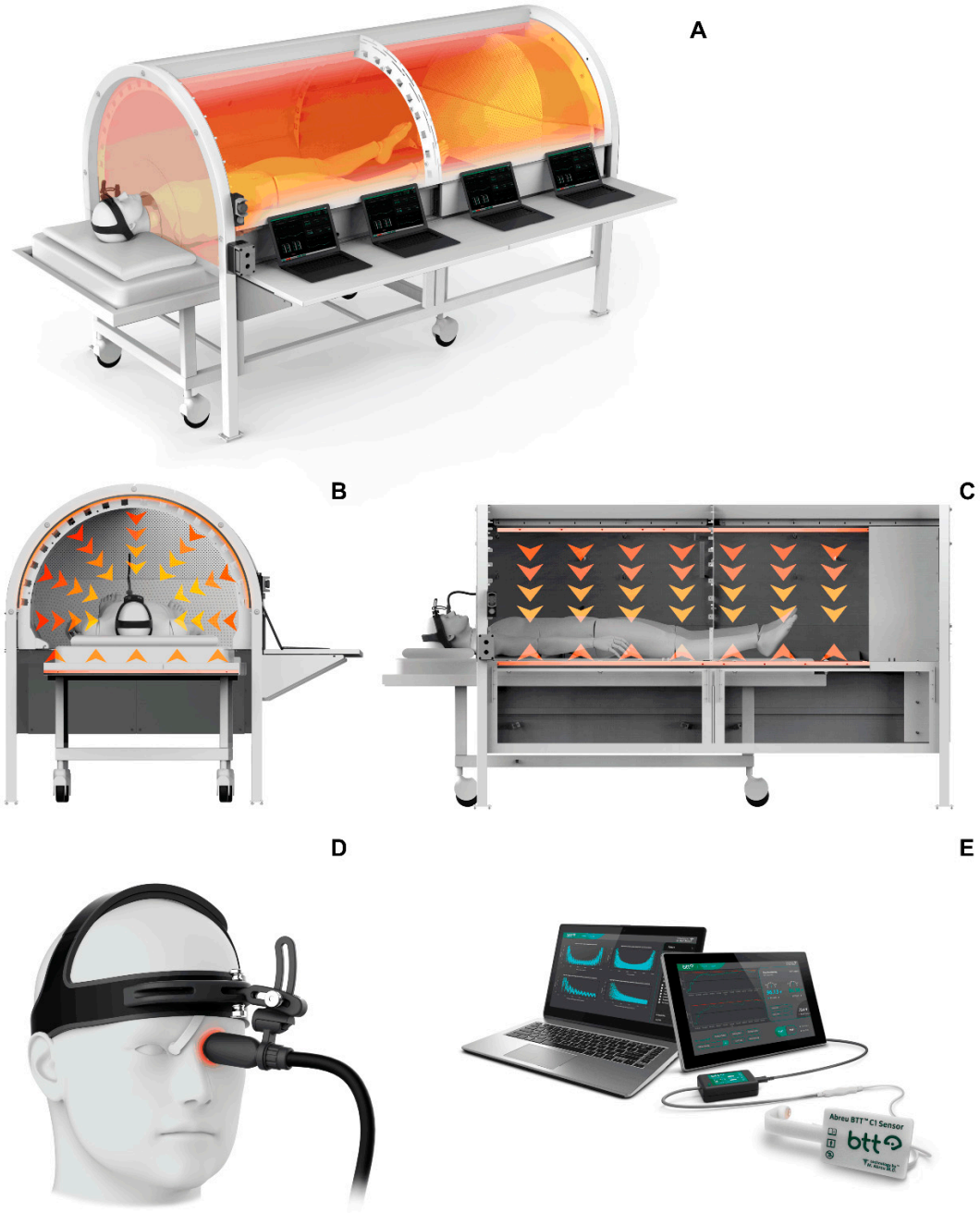

Figure 1. Schematic representation of the structural and functional components of the CBIT² system, a computerized, intelligent thermal delivery via radiative–conductive integration and hypothalamic feedback modulation. (A) Modular structure of the BTT radiant heat chamber, integrated with segments that allow precise control of heat distribution across the body. (B) Frontal and (C) lateral views of the CBIT² chamber, illustrating the direction of heat flow. (D) BTT sensor assembly with an eyelid-mounted BTT thermal inductor. (E) BTT system using the FDA-approved Abreu-BTT 700 System (Brain Tunnelgenix Technologies Corp, Aventura, FL, USA), which integrates the BTT sensor assembly, CBIT² chamber and an eyelid-mounted BTT thermal inductor. BTT: Brain–Eyelid Thermoregulatory Tunnel; CBIT²: Computerized Brain-Guided Intelligent Thermofebrile.

The hot stage (or peak phase) in CBIT² is maintained for approximately 15 to 30 minutes, eliminating the need for prolonged febrile-like state while preserving and even enhancing the efficacy of the thermofebrile response. The final stage is the resolution phase, characterized by a gradual and

 doi:10.20944/preprints202509.0342.v1

controlled decline in temperature, which mimics the natural defervescence seen in malarial fever and marks the therapeutic completion of the induced therapeutic fever cycle. Dr. Wagner-Jauregg's treatment sessions were typically administered continuously over a span of 4 to 8 weeks, resulting in an average of 21 febrile paroxysms. In contrast, CBIT² replicated the core thermal dynamics of malariotherapy with two treatments with an 8-week interval between sessions.

The CBIT² protocol delivers therapeutic fever using a dual-source heating architecture that integrates both radiant and conductive thermal modalities. The treatment chamber employs far-infrared radiative panels to deliver surface-directed heat, while conduction is achieved through a temperature-regulated thermal cover that applies heat directly to the skin. To ensure precise regulation of core and brain temperatures, the CBIT² algorithm also continuously monitors tympanic membrane temperature along with six peripheral surface sensors positioned at key anatomical sites. These multisite thermal inputs, including cutaneous responses, are processed in real time to anticipate hypothalamic counter-regulatory mechanisms, as reflected by sympathetic activation or inhibition resulting in vasoconstriction or vasodilation of cutaneous blood vessels.

This closed-loop feedback system synchronizes thermal delivery with hypothalamic thermoregulatory activity, enabling safe and effective induction of therapeutic fever while modulating hypothalamic driven cooling reflexes. When peripheral vasodilation is detected, interpreted as a potential onset of hypothalamic-mediated cooling reflexes, the algorithm responds by increasing hypothalamic stimulation through modulated thermal delivery, promoting vasoconstriction. This dynamic adjustment enhances heat retention and maintains upward thermal momentum toward the target fever range. In this way, CBIT² leverages the natural thermal effector loop to reinforce rather than oppose fever induction, resulting in precise, sustained elevation of brain temperature without triggering counterproductive autonomic responses.

This bidirectional thermal feedback architecture, combining far-infrared radiation with conduction-based skin heating, enables precise induction of therapeutic fever while prioritizing patient safety. As a result, CBIT² achieves a sustained and regulated elevation in brain temperature within a narrow therapeutic window, preserving the physiological benefits of malarial fever without its associated risks or the need for anesthesia. Throughout the treatment, key physiological parameters are monitored, including blood pressure, heart rate and oxygen saturation, in addition to blood glucose levels to ensure metabolic stability. Hydration is managed through intravenous infusion of sodium chloride or Ringer's lactate. Maintenance of alertness was confirmed by repeated conversation. All CBIT² were administered by the first author (MMA), who is a licensed medical doctor, in his private practice at the BTT Medical Institute in Aventura, Florida, in compliance with the State of Florida and the U.S. FDA regulations.

2.2. Timeline of Treatment Sessions and Objective Assessments

The patient underwent a CBIT² on January 29, 2025 and approximately two months later on March 19, 2025. Clinical and molecular measurements were collected at defined intervals to capture both acute and cumulative effects of CBIT². Baseline values (pre1) were obtained one day prior to the first treatment. Follow-up measurements were taken 24 and 48 hours later, with the 48-hour value designated post1 and the treatment effect calculated as post1 – pre1. A second baseline (pre2) was recorded one day before the second treatment, approximately two months later, allowing evaluation of changes during the inter-treatment interval (pre2 – post1). Measurements 24 and 48 hours after the second session yielded the value post2, which was used to assess both the effect of the second treatment (post2 – pre2) and the cumulative impact of both sessions (post2 – pre1).

Objective testing assessed before (pre1 and pre2) and after (post1 and post2) included the following groupings: upper extremity muscle strength and function; lower extremity muscle strength; stability and balance; and oropharyngeal strength. Biomolecular markers are detailed below. To facilitate assessment of changes within and among phases, %Δ was determined for each parameter. Although all objective tests and measurements were performed before and after the first CBIT² session, not all were performed before and after the second session (primarily due to

 doi:10.20944/preprints202509.0342.v1

scheduling limitations). In addition to the objective determinations, clinical assessments included a written report by the patient and her therapist.

3. Follow-Up and Outcomes

The patient was closely monitored throughout the treatment period and during the six months follow-up phase (up to the current date of 27 August 2025) to assess both clinical and functional responses to the intervention. The results detailed below summarize the short- and medium-term effects observed after each treatment session and during the intersession interval.

3.1. Upper Extremities Strength and Function

Quantitative assessments of upper extremities strength and function before and after two sessions of CBIT² therapy are detailed in Table 1.

Table 1. Quantitative evaluation of upper extremities strength and function before and after two CBIT² sessions.

Upper Extremity Testing	1st CBIT²			2nd CBIT²			
	Pre1	Post1	%Δ	Pre2	Post2	%Δ	%ΔTotal[a]
L arm curls (total #)	10.0	30.0	200.0%	20.0	36.0	80.0%	260.0%
R arm curls (total #)	15.0	26.0	73.3%	20.0	34.0	70.0%	126.7%
L arm curls (#/30 s)	7.0	9.0	22.2%				
R arm curls (#/30 s)	8.0	9.0	11.1%				
Sustained L palmar holding of 1-lb weight (s)	102.0	187.0	83.3%	171.0	190.0	11.1%	86.3%
Sustained R palmar holding of 1-lb weight (s)	112.0	140.0	25.0%	105.0	215.0	104.8%	92%
Sustained L hand pinching (holding) 2-lb weight (s)	96.0	136.0	41.7%	108.0	154.0	42.6%	60.4%
Fatigue of R arm grip (dynamometer units)	30.1	37.4	24.3%	35.8	38.1	6.4%	26.6%

[a] Cumulative impact of both sessions (post2 – pre1). L, left; S, seconds; R, right.

3.1.1. Number of Left and Right Arm Curls

The number of repetitive left and right arm curls with 5-lb weights (shown in Videos S1 and S2) improved following the first CBIT² session. Notably, left arm performance increased from 10 curls during pre1 to 30 curls during post1, representing a 200% improvement. Upon reassessment two months later, approximately half of the initial improvement persisted, with the patient performing 20 curls at pre2. The second CBIT² caused further improvement, with post2-pre2 = 36–20 = 16 curls, such that %Δpost2-pre2 = 80%; and cumulative %Δpost2-pre1 [100 x (36-10)/10] = 260% improvement.

Similarly, the right arm demonstrated improvement after each treatment. After the first treatment, the number of curls increased from 15 to 26 repetitions, representing a 73.3% gain (%Δpost1-pre1). Upon reassessment two months later, only 23.1% of this improvement was lost (%Δpre2-pre1), thereby indicating that more than three fourths of the initial improvement persisted over the ensuing two months. The second treatment caused further improvement, with post2-pre2 = 34–20 = 14 curls, such that %Δpost2-pre2 = 70%, with a cumulative improvement of 126.7% relative to baseline (%Δpost2-pre1).

In addition, we retrospectively viewed counts during the first 30 seconds of the videos obtained before and after the first session in the context of average normal values (between 12 and 17 curls/30

 doi:10.20944/preprints202509.0342.v1

seconds) for 60-79 year-old females during senior fitness testing. Prior to the first session, the patient completed 7 curls/30 seconds with the left arm using a 5-lb weight, which was below the normal range, increasing to 9 curls/30 seconds after treatment (post2-post1 = 2 curls/30 seconds), which constituted a 22.2% improvement (Table 1). The rate of the right arm curls increased from 8 curls/30 seconds to 9 curls/30 seconds; post2-post1 = 1 curl/30 seconds, which constituted an 11.1% improvement. Videos were not obtained for the second session.

3.1.2. Sustained Palmar Holding of 1-lb Weight

Patient's ability to hold a 1-lb weight with an extended left hand (palm facing upward) improved from 102 to 187 seconds, representing an 83.3% improvement (%Δpost1-pre1; Video S3). Upon reassessment two months later, about 67.6% (%Δpre2-pre1) of the improvement persisted, with the patient performing 171 seconds at pre2. The second treatment caused further improvement, with post2-pre2 = 19 seconds, such that %Δpost2-pre2 = 11.1%, and cumulative gain of 88 seconds (post2-pre1), representing 86.3% improvement (%Δpost2-pre1).

The patient's ability to hold a 1-lb weight with an extended right hand increased from 112 to 140 seconds after the first session, representing a 25.0% improvement (%Δpost1-pre1). Upon reassessment two months later, none of the improvement persisted, and performance declined to 105 seconds at pre2, such that %Δpre2-pre1 = 6.3% reduction of function. The second treatment caused further improvement, with post2-pre2 = 110 seconds, resulting in a 104.8% gain (%Δpost2-pre2) and a cumulative 92.0% (%Δpost2-pre1) overall improvement.

3.1.3. Sustained Pinching (Holding) of 2-lb Weight

The patient's capacity to pinch and hold a 2-lb weight (tested for left arm only) increased from 96 to 136 seconds (%Δpost1-pre1 = 41.7% improvement) after the first session (Video S4). Upon reassessment two months later, slightly less than one-third of the increase persisted: pre2 = 108 seconds, such that %Δpre2-pre1 = 12.5 % improvement.

The second treatment caused further improvement, with post2-pre2 of 154–108 = 46 seconds, such that %Δpost2-pre2 = 42.6% after the second session. The second treatment led to a cumulative post2-pre1 = 58 seconds and %Δpost2-pre1 = 60.4% overall improvement.

3.1.4. Maintenance of Grips

Resistance in the fatigue of grip test (right arm only) increased from 30.1 to 37.4 dynamometer force units after the first session (%Δpost1-pre1= 24.3% improvement). Upon reassessment two months later, 18.1% of this initial gain was maintained (%Δpre2-pre1), such that pre2 = 35.8 units. The second treatment caused further increase, with an additional 2.3 units (post2-pre2=38.1–35.8), such that %Δpost2-pre2 = 6.4%, resulting in a cumulative gain of 26.6% (%Δpost2-pre1) in fatigue resistance relative to baseline (for details, see Table 1).

3.2. Lower Extremities Agility, Balance and Gait

Table 2 presents the quantitative assessment of lower extremity agility, balance, and gait before and after two CBIT² sessions.

Table 2. Quantitative assessment of lower extremities agility, balance, and gait before and after two CBIT² sessions.

Lower Extremity Testing	1st CBIT²			2nd CBIT²			
	Pre1	Post1	%Δ	Pre2	Post2	%Δ	%ΔTotal[a]
Duration of R seated leg elevation with 10 lb weight (s)	129.0	187.0	45.0%				
Duration of L seated leg elevation with 10 lb weight (s)	223.0	300.0	34.5%				
Time required to turn in bed (s)	63.0	36.0	-42.9%				

 doi:10.20944/preprints202509.0342.v1

COP area during FAEO (mm²)	33.0	28.0	-15.2%	48.0	46.5	-3.1%	40.9%
COP area during FTEO (mm²)	130.0	74.0	-43.1%	116.0	82.5	-28.9%	-36.6%
COP area during FTEC (mm²)	376.0	345.0	-8.2%	209.0	124.0	-40.7%	-64.1%
COP velocity of sway during FTEC (mm/s)	23.4	17.7	-24.4%	20.0	15.0	-25.0%	-35.9%
COP total excursion during FTEC (mm)	350.0	266.0	-24.0%	300.0	226.0	-4.7%	-35.4%
Average step length (cm)	24.56	29.73	21.05%				
Average stride length (cm)	49.33	59.18	19.97%				
Average gait speed (m/s)	0.41	0.48	17.07%				

[a] Cumulative impact of both sessions (post2 – pre1). COP, center of pressure; FAEO, feet apart and eyes open; FTEO, feet together with eyes open; FTEC, feet together with eyes closed; L, left; S, seconds; R, right.

3.2.1. Sustained Seated Leg Raise Elevation

Seated leg raises with a 10-lb weight (Videos S5 and S6) demonstrated endurance time improvements from 129 to 187 seconds for the right leg (%Δpost1-pre1 = 45% improvement) and from 223 to 300 seconds (34.5% improvement) for the left leg (Table 2). Assessments of leg raises were not performed before or after the second treatment.

3.2.2. Ability to Turn in Bed

Prior to treatment, the patient required 63 seconds to turn from one side to the other in bed (Video S7, Table 2). Following treatment, the time required for turning decreased to 36 seconds, representing a 42.9% (%Δpost1-pre1) improvement. Repeat assessment was not performed before or after the second treatment.

3.2.3. Center of Pressure (COP) Assessment of Postural Sway

A quiet stand test was conducted using the VALD Force Deck system to assess the patient's stability and balance with respect to the center of pressure (COP) at the point of application of the ground reaction force. As summarized in Table 2, the total COP ellipse area, which is a marker of postural sway, was measured during quiet standing under three progressively challenging sensory and biomechanical conditions: feet apart and eyes open (FAEO), feet together with eyes open (FTEO), and feet together with eyes closed (FTEC).Our results revealed that the patient exhibited greater instability as sensory and biomechanical challenges increased, as evidenced by the progressive increase in COP ellipse area from FAEO to FTEC in the pre-treatment assessment (Figure 2A).

Baseline sway was greatest during FTEC due to narrow base of support (FT) and absence of visual input (EC), consistent with the patient's history of positive Romberg test. During FTEC, the first treatment was accompanied by a reduction of area of sway from 376 mm² to 345 mm²; correspondent to an 8.2% (%Δpost-pre1) improvement. During reassessment two months later, the patient evidenced greater improvement: pre2 = 209 mm², a 44.4% improvement from baseline (%Δpre2-pre1). The second treatment caused further improvement during FTEC, as evidenced by a reduction of 85 mm² of sway (post2-pre2), representing a 40.7% (%Δpost2-pre2) gain and a cumulative overall improvement of 64.1% (%Δpost2-pre1).

Changes during FAEO and FTEO are also provided in Table 2 and Figure 2A. As expected, these conditions revealed less initial compromise than FTEC. However, as calculated below, they had greater relative improvement than the 8.2% decline in COP area observed in FTEC during the first CBIT² treatment. During FAEO, area of sway decreased from 33 mm² to 28 mm² (%Δpost1-pre1 = -15.2%), and during FTEO, area decreased from 130 mm² to 74 mm² (%Δpost1-pre1 = -43.1%).

Considering the patient's history of nystagmus and findings of visual-spatial dysfunction and improvement thereof (noted during assessment below), it is not surprising that the first treatment had a greater relative impact on the combination of FT and EO as treatment improved two forms of dysfunction [altered balance (FT) and visual-spatial dysfunction (EO)].

 doi:10.20944/preprints202509.0342.v1

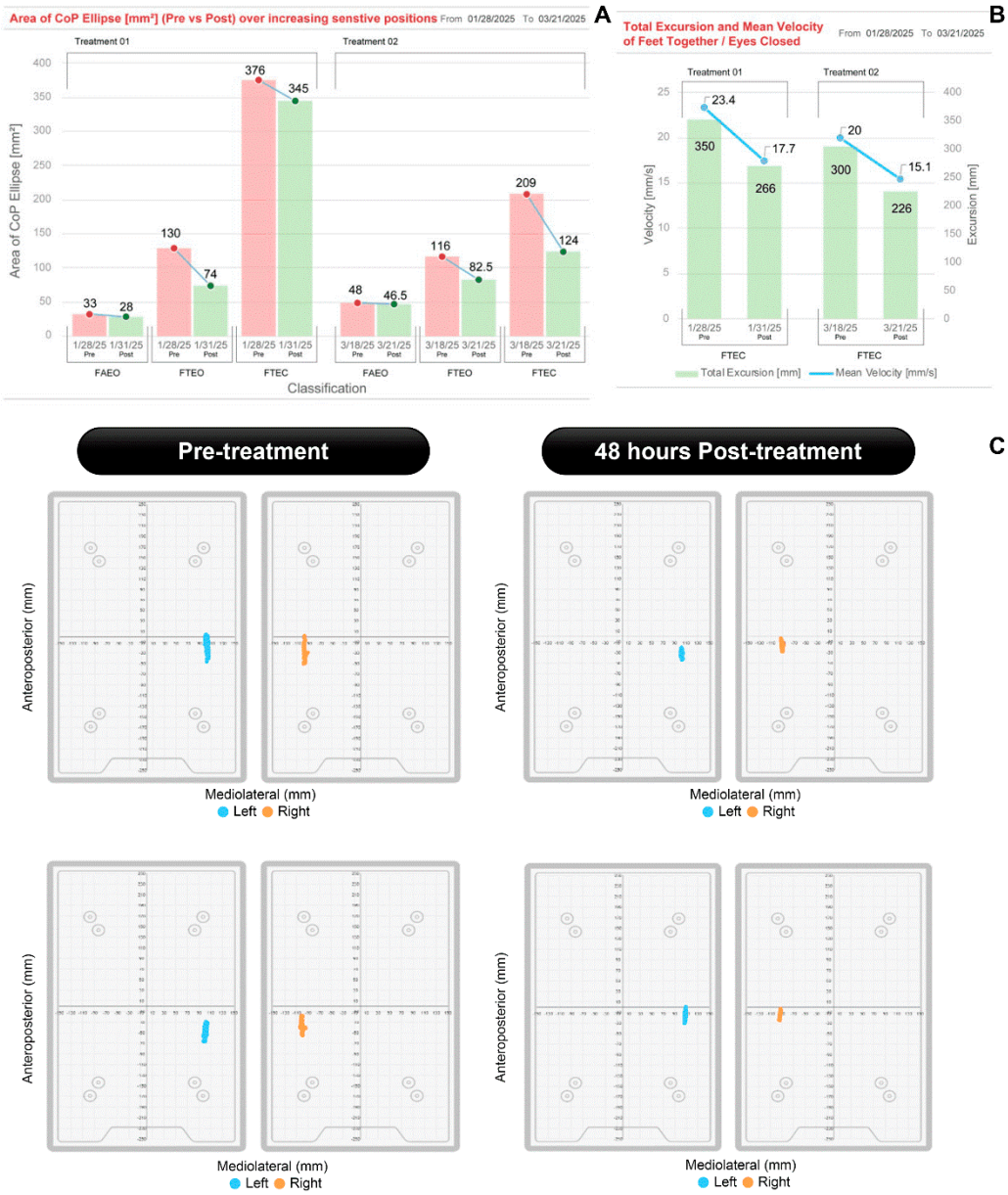

Figure 2. Postural stability and balance improvement following CBIT² intervention with respect to the center of pressure (COP) at the point of application of the ground reaction force. (A) Cumulative bar graphs representing the area of COP ellipse (mm²) over increasing sensory and biomechanical challenges (FAEO, FTEO, FTEC), assessed pre- and post-treatment session. The figure demonstrates that as the challenges in the test increase, the area of COP ellipse also increases. CBIT² treatment reduces the area of COP ellipse, even under increased postural challenge (FTEC condition). (B) Total excursion (mm) and mean velocity (mm/s) of COP during session with FTEC, illustrating a reduction in both parameters. (C) Area of total excursion tracking on force deck [left(blue)/right(orange)] during the entire duration of test, pre and 48 hours post treatment, depicting visually the markedly reduced area of excursion in both sides after the first (upper panel) and second (lower panel) CBIT² treatment. FAEO: feet apart and eyes open; FTEO: feet together with eyes open; FTEC: feet together with eyes closed; CBIT²: Computerized Brain-Guided Intelligent Thermofebrile Therapy.

 doi:10.20944/preprints202509.0342.v1

Additional values due to the second treatment are provided in Table 2. Note that, although FAEO decreased during each of the sessions, it increased in the interval between them, consistent with inhibition of, but nonetheless persistence of, a progressive disorder after a single CBIT² treatment. The optimum number of CBIT² sessions remain to be determined.

3.2.4. COP Velocity and Excursion

As shown in Table 2, additional measurements during testing with FTEC showed that CBIT² treatment caused reductions of COP velocity and excursion (Figure 2B,C). After the first treatment, mean COP velocity decreased from 23.4 mm/s to 17.7 mm/s, representing a 24.36% improvement. After both treatments, the mean COP velocity further decreased to 15.0 mm/s (with %Δpost2-pre1 = 35.9% overall improvement).

With respect to total excursion distance, values decreased from 350 mm to 266 mm after the first treatment (24.0% improvement). After both treatments, overall reduction of total excursion distance was to 226 mm (with %Δpost2-pre1 = 35.4% improvement).

3.2.5. Gait

Gait measurement and analysis before and after the first treatment conducted using ProtoKinetics Zeno™ Walkway Gait Analysis System (Video S8 and S9) provided further objective confirmation of underlying compromise of stability and balance (Figure 3).

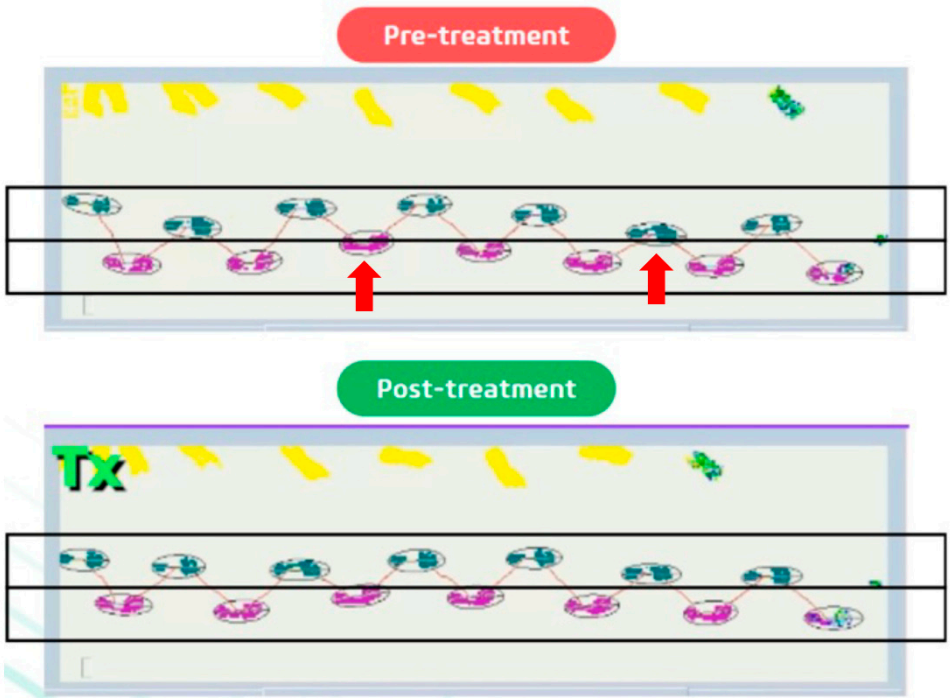

Figure 3. Gait analysis of straight-line walking before and after CBIT² treatment. Prior to treatment, both the right foot (purple) and the left foot (green) crossed the midline. Following treatment, gait restoration was evident, as neither foot crossed the center midline, indicating improved stability and alignment. CBIT²: Computerized Brain-Guided Intelligent Thermofebrile Therapy.

Measurements prior to the first treatment revealed that patient step length, stride length and gait speed were all below the range of normative data. As summarized in Table 2, the first CBIT² treatment resulted in: increase of average step length from 24.56 cm pre1 to 29.73 cm post1, a 21.0% improvement; increase of average stride length from 49.22 cm pre1 to 59.18 cm post1, a 20.0% improvement; and increase of gait speed from 0.41 m/s pre1 to 0.48 m/s post1, a 17.1% improvement.

 doi:10.20944/preprints202509.0342.v1

As seen in Figure 3, pretreatment gait analysis revealed significant lateral instability, characterized by pronounced swaying and deviation of both the right foot (pink trajectory) and left foot (green trajectory), which crossed the central line (indicated by arrows) during ambulation (Figure 3, upper panel). Post-treatment assessment demonstrated marked improvement in dynamic balance, with the patient maintaining a stable, centered trajectory along a straight line as neither foot crossed the central line (Figure 3, lower panel). Enhanced postural control and reduced lateral deviation were evident, reflecting improved muscular function, neuromuscular coordination and gait symmetry following CBIT² intervention. Gait analysis was not performed in association with the second CBIT² session.

3.2.6. Lower Extremity Agility

Additional lower extremity assessments revealed marked improvements in daily activities. Prior to treatment, the patient was unable to perform the cross-leg (ankle-to-knee) test (Video S10) or walk on her toes (Video S11). Following treatment, she was able to complete both the cross-leg test and the walk-on-toes test, indicating enhanced strength and motor coordination. Moreover, dorsiflexion, which had been challenging, became easier, allowing patient to lift her feet higher, with greater ease and approximately doubling of range of motion (Video S12).

3.3. Oropharyngeal and Pulmonary Assessments

3.3.1. Muscles for Swallowing and Speech

Three Iowa Oral Performance Instrument (IOPI) parameters were assessed before and after the first CBIT² session (Videos S13 to S15) to assess muscles essential to the ability to swallow and prevent aspiration as well as to speak. As summarized in Table 3, anterior tongue endurance increased from 19 seconds to 58 seconds after the first session, corresponding to a 205.3% improvement. Posterior tongue endurance improved from 18 seconds to 30 seconds (%Δ = 66.7% improvement). Left-side lip strength increased from 20.2 kPa to 23.75 kPa (17.6% improvement). These findings suggest that CBIT² treatment significantly improved functions essential for swallowing, speech, and eating, consistent with reports by patient and her caregiver in their written summary (below).

Table 3. Comparison of oropharyngeal assessments before and after two CBIT² sessions.

Oropharyngeal Parameters	1st CBIT²			2nd CBIT²			
	Pre1	Post1	%Δ	Pre2	Post2	%Δ	%ΔTotal[a]
IOPI: anterior tongue endurance (s)	19.0	58.0	205.3%				
IOPI:posterior tongue endurance (s)	18.0	30.0	66.7%	43	33	-23.3%	83.3%
IOPI: left lip strength (kPa)	20.2	23.75	17.6%				

[a] Cumulative impact of both sessions (post2 – pre1). IOPI, Iowa Oral Performance Instrument.

IOPI monitoring before and after the second CBIT² session was limited to assessment of posterior tongue endurance. Upon reassessment two months after the first treatment, posterior tongue endurance was 43 seconds, indicating a 43.3% (pre2-post1) increase during the intersession interval. The second treatment led to a decrease in posterior tongue endurance from 43 seconds to 33 seconds, representing a 23.3% decline (%Δpost2-pre2). Overall, CBIT² treatment resulted in a cumulative 83.3% improvement.

3.3.2. Pulmonary Function

Spirometry was performed in recognition of the progressive impact of ALS on respiration, most notably progressive life-threatening compromise of the diaphragm and intercostal muscles. Forced vital capacity (FVC), which is the volume of forced exhalation after a deep breath, and FEV1, which

 doi:10.20944/preprints202509.0342.v1

is volume exhaled as rapidly as possible in one second, were measured during pre1, post1, pre2 and post2 testing; and their ratio (FEV1/FVC%) was calculated (Table 4).

Table 4. Pulmonary function assessments before and after two CBIT² sessions, and at 5-month follow-up.

Pulmonary Parameters	1st CBIT²			2nd CBIT²				
	Pre1	Post1	%Δ	Pre2	Post2	%Δ	%ΔTotal[a]	Follow-Up
FVC (liters)	2.81	3.12	11.03%	2.96	3.00	1.4%	6.8%	3.07
FEV1 (liters)	2.36	2.44	3.39%	2.34	2.40	2.6%	1.7%	2.53
FEV1/FVC (%)	84.10	78.30	-6.90%	79.20	80.20	1.3%	-4.6%	82.0

[a] Cumulative impact of both sessions (post2 – pre1). FEV1, Forced Expiratory Volume in 1 second; FVC, Forced vital capacity.

FVC, a commonly recommended test for assessing ALS progression and severity because it reflects diaphragm and chest muscle strength, was 2.81 liters upon initial baseline (pre1) spirometry. This was below the lower boundary of ~3.2 liters for normal FVC in subjects in same sex and age group, but it fortunately was above the ~80% cutoff commonly considered ominous in ALS. Improvement in FVC after the first treatment was evidenced by increase to 3.12 liters at post1 (an 11.3% improvement). Upon reassessment two months later, FVC was 2.96 liters, indicating that approximately half of the initial improvement persisted (pre2-post1 = 2.96–3.12 = -0.16 liters).

The second treatment showed a small increase in FVC, reaching 3.00 liters. This increase corresponded to an additional 0.04 liters (post2-pre2), representing a 1.4% (%Δpost2-pre2) gain and a cumulative overall improvement of 6.8% (%Δpost2-pre1) relative to baseline, as opposed to the typical progressive decline of this vital indicator of ALS severity.

As shown in Table 4, the change in FEV1 from 2.36 liters at pre1 to 2.40 liters at pre2 constituted an overall %Δ of 1.7%. The baseline value for FEV1/FVC% was 84.1%, which was within the typical range of 75% to 85%. The ratio decreased from 84.1% at pre1 to 80.2% at post2, representing an overall decline of 4.6%.

At the 5-month follow-up, comprehensive pulmonary function testing conducted by the Northwestern University, Chicago, IL, demonstrated sustained or further improved respiratory performance, as evidenced by increases in both FVC (from 2.81 L at baseline to 3.07 L at follow-up) and FEV1 (from 2.36 L at baseline to 2.53 L at follow-up) values. The FEV1/FVC ratio rose slightly from 80.2% (post2) to 82.0% and remained within normal physiological limits, indicating proportional preservation between volume and flow. Overall, these follow-up findings suggest that the respiratory improvements observed after CBIT² were not only maintained but, in certain parameters, continued to improve several months after treatment.

The increase in pulmonary function attributable to CBIT² was consistent with reversing the restrictive nature of ALS-induced muscle weakening as opposed to changes in airway tone.

3.4. Cognitive Function

Cognitive and functional evaluation were performed using the Montreal Cognitive Assessment (MoCA) and ALS Functional Rating Scale (ALSFRS), respectively (Figure 4A,B). MoCA scores demonstrated an improvement from mild cognitive impairment (score of 25) to normal cognitive function (score above 27) after the first treatment, indicating cognitive restoration (Figure 4C). Prior to treatment, the patient exhibited deficits in visuospatial/executive function, as evidenced by difficulties in correctly positioning hands of a clock (ten minutes past 11) and copying a cube (Figure 4C), and compromised recall (of five words). After the first treatment, the patient accurately drew the hands of the clock and the cube and successfully recalled all five words. After the second treatment, her score increased from 27 to 28 between pre2 and post2. The maintenance of the improvement

 doi:10.20944/preprints202509.0342.v1

between post2 and pre1 was consistent with the past the patient's self-reported improvement at the end of the inter-treatment interval.

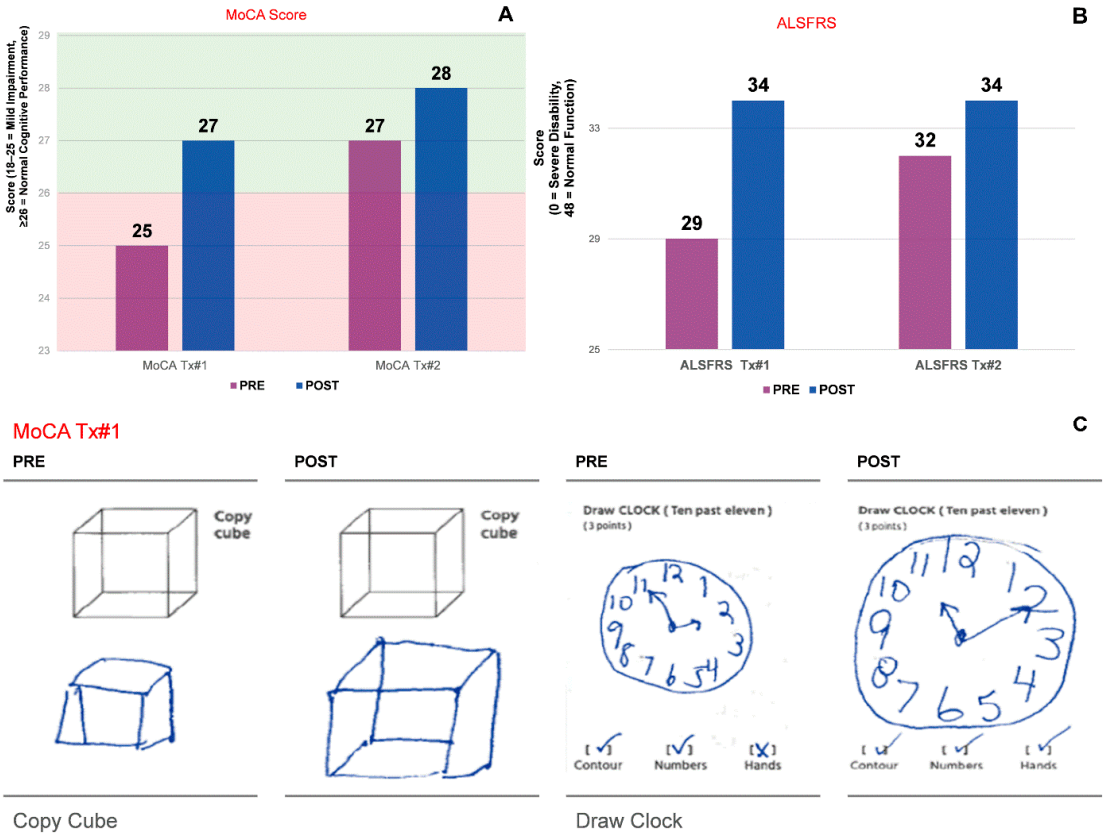

Figure 4. Cognitive and functional improvements following CBIT² treatment as assessed by the Montreal Cognitive Assessment (MoCA) and ALS Functional Rating Scale (ALSFRS). A) Changes in MoCA total scores before and after two CBIT² treatment sessions. In the first CBIT² session, scores increased from 25 at pre-treatment, consistent with mild cognitive impairment, to 27 at post treatment. In the second session, scores increased from 27 at pre-treatment to 28 at post treatment, indicating normalization and subsequent incremental improvement of overall cognitive performance. B) Changes in ALSFRS-R scores also improved progressively across the two treatment sessions, indicating enhanced and maintained overall functional performance. C) The figure illustrates an improvement in the ability of the brain to process and interpret visual information in relation to space following CBIT² session. Pre-treatment, the patient displayed geometric distortion in cube copying and incorrect clock hand placement, suggesting a visuospatial deficit. After treatment, the patient displayed appropriate structural and spatial accuracy and improved handwriting, with resolution of handwriting resembling micrography previously evident in the clock-drawing and cube-copying tasks. ALS: Amyotrophic Lateral Sclerosis; CBIT²: Computerized Brain-Guided Intelligent Thermofebrile Therapy. Tx#1: First treatment session; Tx#2: Second treatment session.

3.5. ALS Functional Rating Scale Cumulative Score

In addition, the patient was assessed according to the 12 functional measures across four domains (bulbar function, respiratory function, gross motor function, and fine motor function) of the ALSFRS. Speech, salivation, swallowing, handwriting, cutting food and handling utensils, dressing and hygiene, turning in bed, walking, climbing stairs, dyspnea, orthopnea and respiratory insufficiency each was rated on a 0 (worst) to 4 (best) scale, such that maximum score was 48. As assessed by the nurse performing the testing, the patient exhibited an ALSFRS score of 29 prior to the first CBIT² session, which increased to 34 after the first session, representing a 17.2% improvement in

 doi:10.20944/preprints202509.0342.v1

functional capacity. The most notable gains were observed in the scores for speech, swallowing, eating, turning in bed, and walking. Pre2 and post2 ALSFRS assessments were performed and showed maintenance of the functional gain.

3.6. Hearing Function

Assessment of hearing with automated testing of auditory sensitivity (GSI AMTAS) showed that there was recovery of sensorineural hearing loss that was affecting the patient's left ear (Appendix B). The pre-treatment audiogram revealed that, while the right ear exhibited normal hearing, the left ear demonstrated mild sensorineural hearing loss. Following the first treatment, both ears were within normal limits.

3.7. Molecular Measurements

Three biomarkers associated with ALS severity, along with a class of stress proteins, were measured. All measurements were performed by independent third-party commercial laboratories. Changes in each biomarker related to ALS severity are shown in Figure 5.

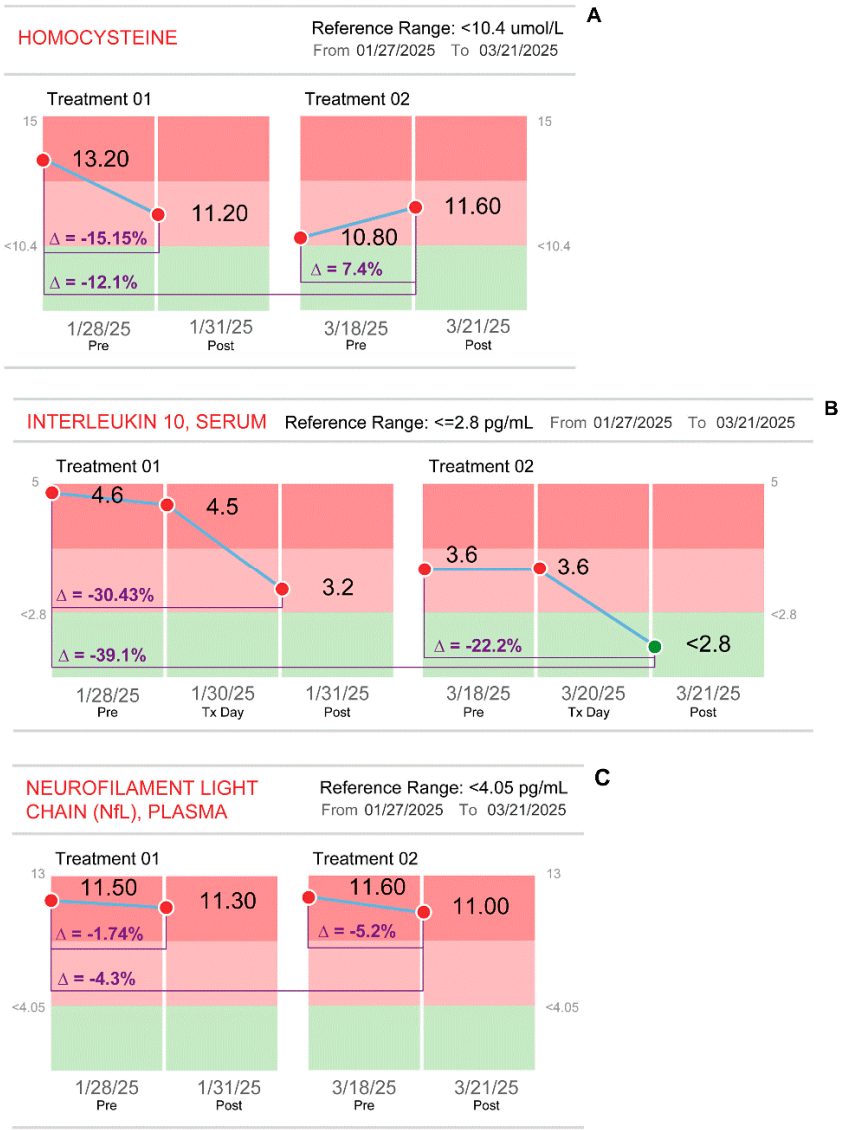

Figure 5. Changes in biomarkers associated with ALS severity before and after two CBIT² treatment sessions. (A) Homocysteine levels demonstrated an overall downward trend across sessions, ranging from 13.20 μmol/L

 doi:10.20944/preprints202509.0342.v1

at baseline (pre-treatment) to 11.60 µmol/L after the second CBIT² session, although values remained slightly above the reference range (<10.4 µmol/L). (B) Interleukin-10 (IL-10) levels showed progressive reductions, declining from 4.6 pg/mL at baseline (pre-treatment) to values within the reference range (<2.8 pg/mL) after the second CBIT² session. (C) Neurofilament light chain (NfL) levels declined across both sessions, decreasing from 11.50 pg/mL at baseline (pre-treatment) to 11.00 pg/mL after the second CBIT² session, although values remained above the reference range (<4.05 pg/mL). The figure also represents the variation (delta values) between the pre- and post-treatment measurements for both sessions, in addition to the cumulative difference from baseline to the post2 treatment session. ALS: Amyotrophic Lateral Sclerosis; CBIT²: Computerized Brain-Guided Intelligent Thermofebrile Therapy; Tx Day: treatment day.

3.7.1. Homocysteine Levels

Homocysteine (normal plasma level <10.4 µmol/L) decreased from 13.2 µmol/L to 11.2 µmol/L after the first treatment, such that Δpost1-pre1 of -2.0 µmol/L constituted a 15.2% improvement. The subsequent decline from post1 to pre2 of 0.4 µmol/L (a 3.6% decrease) showed likely continuation of improvement during the two-month interval between treatments, such that the pre2 value was 18.2% lower than the baseline (pre1) measurement. After the second treatment, homocysteine levels increased by 0.8 µmol/L, indicating a 7.4% "worsening" during the second treatment. Nonetheless, the overall decline from pre1 to post2 (13.2 µmol/L to 11.6 µmol/L) constituted a 12.1% improvement (Figure 5A).

3.7.2. Interleukin 10 (IL-10) Levels

IL-10 (normal serum level ≤2.8 pg/mL) decreased from 4.6 pg/mL to 3.2 pg/mL after the first treatment, representing a 30.4% improvement (Δpost1-pre1) The slight increase (0.4 pg/mL) over the next two months (%Δpre1-post1 = 12.5%) showed that most (87.5%) of the initial improvement was maintained. After the second treatment, IL-10 decreased 0.8 pg/mL, corresponding to a 22.2% improvement. The overall (post2-pre1) decline from 4.6 pg/mL to 2.8 pg/mL represented a 39.1% improvement and constituted a reduction of IL-10 to a normal value (Figure 5B). Thus, elevated IL-10, a marker of the inflammatory pathway leading to mortality in ALS, was downregulated post-CBIT², suggesting a potential shift away from fatal progression for the patient.

3.7.3. Neurofilament Light Chain (NfL) Levels

Neurofilament light chain (normal <4.5 pg/mL) decreased from 11.5 pg/mL to 11.3 pg/mL after the first treatment (%Δpost1-pre1 = -0.2 pg/mL constituted a 1.7% improvement). The increase of 0.3 pg/mL over the next two months (%Δpre2-post1 = 2.7%) indicated that the first treatment did not result in a persistent decline. However, after the second treatment, neurofilament levels decreased by 0.6 pg/mL, indicating a reduction of 5.6% during the second treatment. The overall (post2-pre1) decline from 11.5 pg/mL to 11.0 pg/mL represented a 4.3% improvement (Figure 5C).

3.7.4. Heat Shock Protein 70 (HSP70) Levels

In addition to the biomarkers associated with ALS severity, levels of HSP70 were quantified to assess activation of the cellular stress response pathway targeted by CBIT² therapy. The changes in HSP70 are summarized in Table 5.

Measurement of HSP70 (which has an inconsistent normal range) showed that it increased from 88 pg/mL to 94 pg/mL at 48 hours after the first treatment; post1 48h-pre1 of 6 pg/ml constituted a 6.82% increase. An additional increase of 51 pg/mL over the two-month interval between sessions (%Δpre2-post1 = 54.3%) indicated that the first treatment induced a greater subsequent increase, which persisted for at least two months.

After the second treatment, HSP70 levels decreased by 10 pg/mL (post2-pre2), corresponding to a 6.9% regression during the second treatment. However, the overall difference from pre1 to post2 (47 pg/mL) constituted a 53.4% increase in the HSP70 levels. Potentially confounding assessment of

 doi:10.20944/preprints202509.0342.v1

HSP70 changes, there are multiple variations of this class of proteins, each of which may have a varying time course. In addition to 48-hour HSP70 samples, 24-hour samples were also obtained. The 24-hour value after the second treatment was 126 pg/mL, representing a 13.1% decrease (%Δpost2 24h-pre2) compared to pre2 value. Our findings revealed a peak increase of 64% observed two months after the first treatment session (pre2-pre1).

Table 5. Heat shock protein 70 (HSP70) levels before and after CBIT² treatment.

Molecular measurements	1st CBIT²				2nd CBIT²				
	Pre1	Post1 24 h	Post1 48 h	%Δ	Pre2	Post2 24 h	Post2 48 h	%Δ	%Δ Total[a]
HSP70 (pg/mL) (variable range of "normal")	88.0	97.0	94.0	6.82%	145.0	126	135.0	-6.9%	53.4%

[a] Cumulative impact of both sessions (post2 – pre1). For %Δ, post values were calculated using the 48-hour values; HSP70: heat shock protein 70.

3.8. Electrophysiological Evaluation: Evidence of Cessation of Motor Neuron Death Following CBIT²

Five months after the first treatment (June 24, 2025), electrophysiological studies were repeated by an independent university-based neurologist services and compared by the authors in Table 6 to the pretreatment examination (October 25, 2024) to evaluate changes in motor unit integrity and neuromuscular signaling. The EMG protocol was designed to detect both the silence that accompanies motor neuron death and the reemergence of electrical activity that could signify reinnervation. In this way, the electrophysiological data provided a real-time window into the potential for neuronal restoration, etched into the muscles themselves.

Table 6. Comparison of pre-treatment and post-treatment electromyography.

Parameter	25 October 2024 (Mayo)	24 June 2025 (Northwestern)
Fibrillations	Present (e.g., gastrocnemius) = active motor neuron death	Absent = no more motor neuron death
Positive sharp waves (PSWs)	Present (implied)	Absent
Fasciculations	Present (e.g., tibialis anterior) = motor neuron injury and irritability present	Absent = no more motor neuron injury and irritability
MUAP duration & amplitude	Increased (chronic changes in L4-S1)	Increased (1+ in vastus lateralis, rectus femoris and tongue)
Recruitment pattern	Reduced in multiple muscles	Full in most, mildly reduced in few
Reinnervation Evidence	Yes (chronic reinnervation)	Yes (chronic reinnervation)
Bulbar involvement (Tongue)	No active denervation	No active denervation
Sensory nerve studies	Normal	Normal

 doi:10.20944/preprints202509.0342.v1

Motor nerve studies	Normal	Normal
Disease activity interpretation	Active denervation ongoing, disease progressing, active neurodegeneration	No active denervation consistent with disease reversal and effective therapeutic response

MUAP, Motor Unit Action Potential.

Pretreatment examination performed on October 25, 2024 (see Appendix A1), revealed active denervation, disease progression, and ongoing neurodegeneration, as evidenced by the presence of fibrillations, fasciculations, and chronic denervation changes in muscles innervated by the L4–S1 roots. These results are consistent with active motor neuron loss and increased neuronal injury and irritability. In contrast, results from the EMG conducted five months after the first CBIT² session (Appendix A2) demonstrated the presence of chronic reinnervation in the vastus lateralis, rectus femoris, and tongue, without any signs of active denervation, as indicated by the absence of fibrillations, positive sharp waves, and fasciculations. These findings suggest electrophysiological stabilization, absence of active disease progression, and a positive therapeutic response (Table 6).

3.9. Self-Reported Clinical Improvements

One month after the first treatment, the patient and her physical therapist reported marked improvements in multiple aspects of daily living that were impossible or unachievable before CBIT². These included successfully engaging in challenging and strenuous activities and demonstrating restored endurance and balance. She was able to attend a wedding, where she danced for four hours. The patient also reported that she now walks more frequently and without relying on her walker. She can go up and down the stairs independently, even carrying objects like a book. Getting in and out of bed has become easier, as she can now sit up, roll over, and lift her legs without external assistance. Her ability to perform daily activities has also improved. She reported that it is easier to put on socks, open jars, and grip objects such as a water bottle, a task that was previously challenging due to weakness in her hands. Balance and coordination have improved, allowing her to vacuum, carry objects while walking, and reach for items in the kitchen without difficulty. Shoulder pain, which previously affected her ability to drive, has completely resolved, making driving comfortable again. Patient's speech and swallowing also have shown remarkable progress. She now speaks with greater clarity and projection, with a noticeable reduction in slurring. Her ability to sing has returned, and she is able to sing in the shower and in the car. Chewing and swallowing food was restored. The patient also reported that she regained a greater level of independence in daily tasks, including dressing, eating, and mobility. Food no longer needs to be cut by husband; patient can do it by herself. Remarkably, patient stated that, at church, she kneeled which she has not done in years.

The overall improvement in her quality of life is evident, as she can now participate in social activities, such as attending events and engaging in physical exercise, with increased confidence and energy.

From Paralysis to Playing Golf

Recovery in this ALS case was not limited to incremental improvements in strength or gait but extended to the restoration of complex, high-level motor coordination. Within three months of initiating treatment, the patient advanced from reliance on a walker to playing golf—an activity that requires balance, strength, timing, proprioception, and precise neuromuscular sequencing. One month after the second treatment, she not only performed coordinated swings but also successfully completed golf holes, demonstrating functional integration of motor recovery. This outcome cannot be explained by compensatory adaptation; rather, it signifies the restitution of underlying neuromuscular and cortical control. The ability to transition from paralysis to the golf course parallels the dramatic functional restorations once observed during malarial fever therapy, reinforcing that

 doi:10.20944/preprints202509.0342.v1

reversal—not palliation—of neurodegenerative pathology is possible through brain-guided, reengineered fever therapy.

3.10. Physical Therapy-Assessed Outcomes

During physical therapy evaluations, her strength and stability have improved. She successfully performed bridges on an exercise ball without assistance, demonstrating improved core strength. Her gait is smoother, with reduced stiffness and improved coordination. Tandem balance, floor transfers, and walking endurance have also improved. Physical therapy assessments in Illinois have documented measurable progress in various motor functions, including an increase in tandem balance time, a reduction in the time needed for the Timed Up and Go (TUG) test, and improved gait speed. Her tandem balance test showed an increase in stability, with her right side improving from 23 to 30 seconds and her left side increasing from 8 to 12 seconds. The TUG test – i.e., time it takes to rise from a seated position, walk three meters, turn, walk back, and sit down – improved from 18 to 16 seconds, indicating better movement efficiency. Her gait speed slightly increased, and her straight leg raise (SLR) supine test demonstrated greater flexibility and range of motion. These objective data points reinforce the visible functional progress observed in her daily activities. Her neuromuscular control has improved, leading to more fluid movements and reduced stiffness. Physical therapy results in Illinois, conducted one month after CBT² treatment, confirmed measurable improvements consistent with the tests performed 48 hours post treatment at the BTT Medical Institute in Florida.

4. Discussion

This case report presents the first documented reversal of ALS, a disease long regarded as irreversible and uniformly fatal, achieved through the first application of therapeutic fever to ALS, resulting in neurological, molecular, and electrophysiological reversal of ALS that directly challenges the entrenched view of inexorable progression in ALS. These findings provide historic proof-of-principle that ALS pathology is, in fact, reversible. While this outcome marks an unprecedented turning point in our understanding of ALS, its broader significance must now be tested through rigorous, large-scale clinical trials to confirm reproducibility, durability, and therapeutic potential across the spectrum of misfolding protein disorders including other neurodegenerative diseases.

In 1917, Wagner-Jauregg's case report showed that deliberate fever induction could reverse dementia paralytica, the first proof that fever held curative power for neuropsychiatric disease [15], becoming a breakthrough which was later confirmed by trials and honored with the 1927 Nobel Prize. More than a century later, in that same lineage, the present case report demonstrates that fever, now digitally reengineered and brain-guided through CBIT², can safely restore brain function in ALS, a disease long considered irreversible and fatal.

The BTT-based intelligent programmed fever treatment (formally termed CBIT²) resulted in complete reversal of ALS and restoration of lost brain function. This unprecedented outcome stands in sharp contrast to prevailing expectations for ALS. The Mayo Clinic report, for example, had emphasized the inexorable course of the disease, stressing that *"progressive lower motor neuron denervation is unfortunately inevitable"* and communicated to the patient a life expectancy of only three to five years. This statement underscored the long-established scientific consensus, grounded in decades of rigorous research, that once degeneration begins in ALS there is progressive motor neuron loss, an irreversible decline, and life expectancy limited to only few years. For generations, this has defined ALS as a death sentence, with no path back once denervation sets in. Yet in this case, that inevitability was not only averted but replaced by documented electrophysiological evidence of reversal of denervation, with elimination of fibrillation and fasciculation, demonstrated by irrefutable objective testing with EMG, the gold standard for ALS diagnosis. What science long judged as inexorable decline is here replaced by recovery, proving that the presumed irreversibility of ALS can, in fact, be undone, echoing the Nobel Prize–validated precedent of fever therapy, which a century ago restored brain function in dementia paralytica.

 doi:10.20944/preprints202509.0342.v1

After her initial diagnosis at the Mayo Clinic in Minnesota, the patient was followed in her hometown at Northwestern University, ranked among the leading neurology centers in the United States, where the ALS diagnosis was independently confirmed and she was thus maintained on the FDA-approved drugs for treating ALS riluzole and edaravone. Despite expert care at both of these prestigious centers, Mayo Clinic and Northwestern University, her neurological function declined relentlessly, in keeping with the scientifically established expectation of inevitable progression and death in ALS.

A turning point came when an acquaintance, who had himself been successfully treated at the BTT Medical Institute, urged the patient to seek care in Florida. Following treatment with CBIT² by Dr. M. Marc Abreu at the BTT Medical Institute, she returned to Northwestern for follow-up, where the neurologist who performed the EMG was confronted with the extraordinary reality that the study demonstrated elimination of denervation and fasciculations, providing irrefutable electrophysiological evidence of cessation of motor neuron death and supporting the conclusion of disease reversal. Considering this unprecedented finding, the Northwestern neurologist discontinued all the patient's ALS medications which is an outcome virtually unimaginable for a disease long regarded as irreversible and consistently fatal. Both riluzole and edaravone, prescribed exclusively for ALS, were stopped, reflecting the extraordinary fact that the patient no longer met diagnostic criteria for ALS underscoring the plausibility of cure through programmed fever therapy. That grim prognosis for ALS is no longer a reality: instead of being shackled to a death sentence, the patient here now faces life in abundance, free of ALS, able to dance and even play golf and pickleball, as seen in the videos provided in this report.

In addition to EMG demonstrating that ALS was no longer present, biomarkers shifted toward recovery, with reductions in neurofilament light chain and homocysteine, normalization of IL-10, a cytokine whose persistent elevation as seen in this patient correlates with increased mortality, besides a surge in HSP70 expression. Clinically, she advanced from walker dependence to restored gait, safe swallowing, strengthened respiration, improved speech, and fully normalized cognition. Most strikingly, she regained the ability to perform complex motor tasks once thought irretrievable, such as swimming, walking unaided onto a golf green and sinking consecutive putts as well as returning to active sports.

Findings herein revealed restoration of motor neuron function following BTT-based intelligent programmed fever treatment, which is an outcome that directly contradicts the presumed irreversibility of motor neuron loss. This transformation, once unimaginable, echoes a truth first acknowledged nearly a century ago, when the Nobel Prize Committee recognized malarial fever therapy as the first demonstration of fever's curative power for neuropsychiatric disease. The exceptional ALS reversal achieved here honors the vision, extending it into the modern era through BTT-based brain-guided programmed fever therapy. Nearly a century later, that foundation identified by the Nobel Prize has been extended and reengineered through CBIT², transforming a once-forgotten treatment into a modern, infection-free, computerized intelligent brain-guided fever therapy that culminated in full reversal of ALS, which resulted in the discontinuation of all ALS-specific pharmacologic treatment.

The febrile response was digitally induced using CBIT², a novel, artificial intelligence-enhanced treatment that delivers therapeutic fever safely and precisely through synchronized thermoregulatory modulation using an FDA-approved computerized platform [19]. CBIT² digitally reengineers the curative principle behind the 1927 Nobel Prize–winning malarial fever therapy into a brain-guided, programmable intelligent treatment. This fully noninvasive and unique procedure proved exceptionally safe, with no adverse effects or complications observed during treatment, within the critical 48-hour post-treatment window, or across the entire six-month follow-up, affirming both its safety and durability of therapeutic effect.

By normalizing the inflammatory response and activating the neuroprotective heat shock response, without pharmacologic agents or infectious stimuli, CBIT² provides a molecularly

 doi:10.20944/preprints202509.0342.v1

grounded and clinically actionable strategy for the restoration of motor neurons in ALS, a disease historically defined by relentless progression, therapeutic failure, irreversibility, and fatal outcome.

Malarial fever therapy, initially developed to combat spirochete infection in neurosyphilis through induced fever, earned the Nobel Prize in Medicine in 1927, though its impact on brain pathology was not yet understood at the time. Nevertheless, this fever-based intervention was rapidly validated across Europe for achieving what was once deemed impossible: the reversal of advanced neurological disease, with restoration of both motor and cognitive function in patients with dementia paralytica [10–18]. This disease reversal by malarial fever therapy that was later extensively documented across diverse populations worldwide, emptied asylums once filled with paralyzed patients facing inevitable death, and established, more than a century ago, that brain damage is, in fact, reversible, which is the principle that supports the restoration of brain function in ALS reported here. However, there is a major distinction in the proposed mechanisms. Restoration from malarial fever was historically attributed to the fever-induced death of *Treponema pallidum*. By contrast, Abreu recognized that fever itself was capable of restoring brain function through activation of the heat shock response, a molecular defense that acts directly on misfolded proteins such as TDP-43. The findings described above, and confirmed in our patient, demonstrate that neuronal recovery arises from the direct biomolecular effect of fever-induced heat shock responses acting at the level of injured nervous tissue.

CBIT² represents a paradigm shift from symptom management to disease-modifying therapy that transformed fever into a computer-controlled treatment guided by real-time feedback from the brain's thermoregulatory center. The mechanistic rationale for this unprecedented recovery in ALS lies in hypothalamic-guided induction of the heat shock response. By directly addressing misfolded proteins such as TDP-43, the molecular driver of ALS pathology, CBIT² restores proteostasis and neuronal function via HSP induction. Unlike saunas or conventional hyperthermia, which trigger heat-dissipating reflexes and oppose therapeutic temperature elevation, CBIT² operates in synchrony with hypothalamic pathways via the Brain–Eyelid Thermoregulatory Tunnel, enabling safe, titrated induction of therapeutic fever without adverse effects. This noninvasive approach transforms the hypothalamus from an opponent into the driver of fever, overcoming physiological barriers that have limited prior thermal therapies.

Using continuous, noninvasive monitoring of brain temperature and thermodynamics at the eyelid via the BTT, this intelligent system modulates thermal delivery via a thermal chamber and an eyelid heat inductor to prevent hypothalamic counterproductive cooling mechanisms, maintaining alignment with thermoregulatory response required to induce therapeutic thermofebrile response. CBIT² integrates algorithmically controlled and synchronized delivery of radiative and conductive heat directed by hypothalamic signals through a computerized platform having a sensor assembly, thermal chamber, eyelid heat inductor, and an intelligent closed-loop feedback control (Figure 1). Bidirectional heat exchange in concert with the hypothalamus is achieved by a sensor at the BTT site capturing efferent brain thermal signals while a heat inductor delivers afferent inputs, resulting in a controlled rise and fall in brain temperature, reaching up to 41.6 °C, that replicates the natural cyclic rhythm of malarial fever within a safe, noninfectious therapeutic architecture, which is enabled by the discovery and characterization of the BTT [46].

Emerging molecular evidence unveils a surprising mechanistic bridge between the dramatic recoveries once seen with malarial fever therapy in 1927 and the remarkable restoration of motor neuron function in 2025 observed in ALS following CBIT². Though separated by more than a century and distinct in etiology, neurosyphilis and ALS reveal a striking pathological convergence at the molecular level marked by the accumulation of misfolded proteins forming TDP-43 aggregates [42,43]. This shared molecular pathology reveals disrupted protein homeostasis as a disease mechanism in both neurosyphilis and ALS, suggesting that targeted fever-based modulation may offer an effective treatment to restore neural function. Just as malarial fever therapy reversed motor and cognitive decline in dementia paralytica, the digitally controlled, brain-guided programmed

 doi:10.20944/preprints202509.0342.v1

fever described here restored lost motor and cognitive function in ALS, revealing a molecular mechanism spanning a century of clinical practice.

By eliminating the risks associated with malarial infection including potentially fatal complications such as cerebral malaria caused by parasitic invasion of the brain, CBIT² safely replicates the intensity and cyclic dynamics of malarial fever once used to cure dementia paralytica, transforming this century-old therapy into a noninfectious, titratable, computer-guided intervention. In a single 2.5- to 5-hour treatment session, CBIT² delivers an average of two cycles of thermofebrile activation mimicking malarial fever, consisting of hyperthermia via chamber and fever induction via hypothalamic signaling at the BTT site, dynamically calibrated to the patient's individual hypothalamic thermal signal, thereby avoiding conflict with central thermoregulation while enabling safe induction of programmed thermofebrile response.

Hypothalamic-driven treatment by CBIT² stands in stark contrast to saunas and conventional skin-heating methods—including infrared hyperthermia devices, resistive heating systems, radiant heat panels, far-infrared equipment, infrared therapy beds, heat blankets, and whole-body hyperthermia systems—which act at the skin surface. These approaches stimulate cutaneous thermoreceptors and trigger hypothalamic heat-dissipating reflexes, turning the brain into an opponent, as occurs with saunas, actively fighting against the very temperature elevation required for therapy. In effect, the brain deploys its thermal defenses as a barrier, activating cooling mechanisms, and preventing the safe achievement and maintenance of the core and brain temperatures needed for robust activation of heat shock transcription factors. CBIT² uniquely overcomes this physiological opposition, transforming the hypothalamus from an opponent into the driver of therapeutic fever.

Additionally, hyperthermia methods lacking synchronization with hypothalamic thermoregulation can subject patients to significant physiological distress including dizziness, nausea, vomiting, respiratory compromise, and even loss of consciousness, severe brain thermal injury, and coma [51] as externally applied heat to the body surface conflicts with central thermal signaling. Because unopposed hypothalamic-driven heat dissipation mechanisms counteract heat applied to the skin surface, as occurs with conventional whole-body hyperthermia, achieving therapeutic temperature levels often requires excessive heating, which may lead to complications such as heatstroke, respiratory arrest, and brain injury. Despite their associated physiological burden and significant safety risks, conventional whole-body hyperthermia methods frequently fail to achieve or sustain therapeutic fever temperatures, such as the 41.6 °C observed in malarial fever, primarily due to misalignment with hypothalamic thermoregulatory control. Efforts to mitigate these uncomfortable and potentially serious adverse effects through conventional anesthetics are similarly counterproductive, as these agents disturb thermoregulatory function and are well documented to induce intraoperative hypothermia [52], directly opposing the desired thermal increase for effective heat shock response.

Attempts to achieve therapeutic temperature levels during whole-body hyperthermia for cancer treatment have been constrained by serious safety concerns, including coma resulting from excessive heat exposure compounded by reliance on rectal temperature monitoring [51], a technique known for over a century to inadequately reflect brain temperature [53–57], resulting in undetected cerebral thermal overload and potentially life-threatening complications. In sharp contrast, CBIT² titrates perihypothalamic temperature, using digitally synchronized, hypothalamic-guided modulation to replicate the therapeutic dynamics of malarial fever without triggering defensive cooling responses, enabling a safe, well-tolerated, and effective treatment.

By advancing the Nobel Prize-recognized fever-induced disease reversal with digital precision, CBIT² safely offers a potential treatment not merely to slow but to reverse neurodegenerative processes. In the ALS case presented, reversal was supported by objective improvements in motor function, reductions in disease-associated blood biomarkers, and increased expression of heat shock proteins. The restoration of functional independence and recovery of complex motor tasks, such as dancing, singing, and playing golf, including coordinated swings and successful hole completion, in

 doi:10.20944/preprints202509.0342.v1

the ALS case here suggest reversal of underlying neurodegenerative pathology, closely resembling the total restoration of lost brain function once achieved a century ago with malarial fever therapy [10–18].

A profound impact, with implications for all ALS patients, was revealed electrophysiologically (see Appendix A). Following CBIT², EMG demonstrated the complete absence of denervation across all tested muscles, which is a remarkable finding given that continuous active denervation, prior to BTT-based programmed fever therapy, is a hallmark of ongoing motor neuron death in ALS. The disappearance of both fibrillations and fasciculations previously present provides irrefutable electrophysiological evidence that the pathological process of motor neuron degeneration was eradicated. Moreover, widespread chronic reinnervation changes observed in the absence of denervation confirmed that compensatory mechanisms were active and now proceeding without ongoing neuronal destruction. These electrophysiological results were paralleled by normalization of disease-associated molecular biomarkers and objective neuromuscular recovery, further reinforcing the conclusion that the underlying neurodegenerative process had been reversed. The clinical, molecular, and electrophysiological findings challenge the long-standing view of ALS as an irreversible and fatal condition, suggesting that CBIT² may reactivate the therapeutic principle of malarial fever, first successfully applied to reverse dementia paralytica, and now offering a path to structural and functional brain recovery in ALS.

CBIT² induced significant clinical improvements, supported by objective quantitative measures as well as patient self-report and physical therapist evaluations. These included increased strength in the arms and legs, improved balance and gait, improved bulbar function (enhanced speech, salivation and swallowing), improved fine motor (handwriting, cutting food), coordinated motor (playing golf and pickleball) and gross motor (walking, stair climbing) activity and improved pulmonary capacity, as well as gains in visuospatial function and cognition. Objective assessments confirmed enhanced motor control balance with eyes open (EO) and eyes closed (EC), feet apart (FA) and feet together (FT) (Figure 2), normalized gait (Figure 3), restored cognition (Figure 4), increased tongue endurance and improved speech articulation. These functional improvements were accompanied by a five-point increase in the ALSFRS, sustained over a six-month period, an outcome of particular significance given that the ALSFRS is primarily designed to measure progressive decline, and a sustained increase or stabilization in score is considered both exceptional and clinically meaningful [58]. Notably, even edaravone, an approved drug known for its ability to slow ALS progression by preventing neuronal damage, has not been able to produce a significant difference in ALSFRS-R scores compared to placebo [59]. Although previous studies have demonstrated that a subset of patients with early-stage ALS experienced a slower rate of functional decline with edaravone, they have failed to demonstrate any increase in ALSFRS-R scores [60].

At the biomarker molecular level, the response observed following CBIT² indicates a shift from active neurodegeneration toward neuronal preservation and recovery, reflected in meaningful changes in biomarkers associated with ALS progression and fatal outcome. Blood levels of NfL are considered robust predictors of ALS progression [61], and their reduction, as shown here post BTT-based programmed fever, has been explored as a promising therapeutic target with disease-modifying potential, as exemplified by tofersen, an antisense oligonucleotide recently approved for the treatment of ALS in adults with SOD1 (superoxide dismutase-1) gene mutations [21].

Our results also revealed a striking and unprecedented molecular finding involving normalization of IL-10, a cytokine whose persistent elevation in ALS is a hallmark of relentless neuroinflammation and a harbinger of poor prognosis and mortality [62]. This cytokine normalization (IL-10) followed the second treatment and coincided with a marked increase in HSP70 expression, rising from 6.82% after the first session to 53.4% post-second session. Elevated IL-10 has been inversely correlated with survival in ALS, and its downregulation may signal reduced inflammatory burden and a departure from a fatal disease trajectory post CBIT². Together, the reduction in neurofilament and homocysteine, which are biomarkers associated with neuronal death [61] and poor prognosis in ALS [63], respectively, alongside the normalization of IL-10, provides early

 doi:10.20944/preprints202509.0342.v1

evidence that CBIT² may halt the pathological course of ALS and initiate a process of functional restoration and molecular reversal.

The neuromuscular, molecular, and electrophysiological improvements observed are consistent with a CBIT²-induced rise in heat shock proteins (HSPs). HSPs are molecular chaperones that regulate protein folding, degradation, and cellular stress responses, while preventing the accumulation of neurotoxic aggregates, which are functions that are critically impaired in ALS [64,65]. Among them, HSP70 is especially notable for its neuroprotective and restorative roles, including counteracting misfolded protein toxicity, enhancing cellular resilience to oxidative stress, and facilitating neuronal repair [31,66,67]. The ability to use programmed fever to induce HSP70 noninvasively in a clinical setting represents an unprecedented therapeutic achievement, long considered unattainable, and provides a mechanistic foundation for the reversal of neurodegeneration documented in this case.

ALS reversal aligns with the principle of malarial fever therapy, that we revealed here may have acted at the molecular level by refolding misfolded TDP-43 protein and eliminating toxic aggregates in dementia paralytica. Studies in ALS animal models have shown that exogenous HSP70 administration enhances neuromuscular function and prolongs survival [32,67]. These findings parallel those in the present case, which demonstrated improved neuromuscular performance accompanied by normalization of IL-10 levels, which is a biomarker shift associated with extended survival, as elevated IL-10 has been linked to increased mortality [62]. Upregulation via histone deacetylase inhibitors enhances motor neuron resistance to stress-induced damage [68] and regional differences in HSP expression and inflammation in ALS may influence disease progression [69], supporting the potential of HSP-modulating therapies, as shown here.

The collapse of the cellular stress response in ALS disrupts proteostasis, leading to the accumulation of misfolded proteins and neurotoxic aggregates. In contrast, CBIT² induced a robust upregulation of HSPs, which may restore proteostatic balance by enhancing chaperone-mediated protein folding and promoting the clearance of toxic aggregates. These molecular effects are consistent with the known role of HSP70 in maintaining proteostasis and regulating neuroimmune signaling. Through activation of HSF1, HSP70 suppresses inflammatory cascades involving NF-κB (nuclear factor kappa B) and JNK (c-Jun N-terminal Kinase) [70] besides reducing cytokine production [71] while modulating glial activity by inhibiting pro-inflammatory microglial phenotypes (M1) [72], enhancing anti-inflammatory responses, and reducing astrocyte reactivity [70]. This immunological modulation highlights a broader mechanism by which CBIT² restores immune homeostasis and reverses molecular hallmarks of ALS progression and mortality. The upregulation of endogenous HSPs during CBIT² thus offers a promising avenue for ALS treatment and disease reversal, paralleling malarial fever therapy outcomes that achieved clinical cure in neurosyphilis despite structurally damaged brain tissue harboring misfolded TDP-43, which is also present in ALS, further supporting the plausibility of a cure for ALS.

Clinical studies have tested pharmacological amplification of the heat shock response, such as with arimoclomol, a co-inducer that enhances HSP70 expression. However, despite its mechanistic rationale, arimoclomol failed to provide meaningful clinical benefit in ALS patients and was associated with adverse effects including approximately 29% increase in NfL levels compared with placebo [20], which is in sharp contrast to reduction of NfL observed following CBIT².

We anticipate that the impact of CBIT² on HSP levels will constitute a major therapeutic breakthrough. In this two-session introduction of CBIT², HSP70 increased by 53.4% between pre1 and post2 determinations, reaching a peak increase of 64% two months after the first treatment session. The observation that HSPs in our patient reached their highest at the assessment two months after the first CBIT² treatment is consistent with a multi-step process which includes treatment-induced release of HSF1 which in turn causes DNA-mediated synthesis of HSPs via heat shock element gene. It has been shown in in vitro primary culture ALS models that activation of HSF1 enhances motor neuron survival, reducing protein aggregation and mitigating proteotoxic stress [27].

The prolonged therapeutic impact of CBIT² observed in this case reinforces its biological plausibility and supports the durability of its effect. The heat shock response activated by CBIT² is a

 doi:10.20944/preprints202509.0342.v1

well-established neuroprotective and restorative mechanism, associated with reduced neuroinflammation, enhanced cellular resilience to oxidative stress, and decreased accumulation of misfolded proteins, which are hallmarks of neurodegenerative disease [31,66,67].

In apparent contrast to the known effects of hyperthermia on HSP activity [73], a thoughtfully designed study using a mouse model of ALS reported potential therapeutic effects of chronic intermittent mild whole-body hypothermia [74]. By inducing mild hypothermia through chronic intermittent cooling cycles, investigators observed delayed disease onset, improved neuromuscular junction integrity, and prolonged survival in the mouse model of ALS [74]. They also demonstrated that hypothermia restored levels of HSP70 and other molecular chaperones, further supporting its neuroprotective effects in the mice [74]. The findings further support the rationale for developing thermally-based therapies, both fever and cooling, for neurodegeneration. It remains to be determined how temperature(s) and thermodynamics impact the structural and functional deterioration(s) of ALS. The ability to noninvasively assess brain temperature and hypothalamic responses via the BTT and its correlation with disease activity may help address longstanding questions in ALS pathophysiology. However, species-specific genetic differences, particularly those influencing synaptic connectivity and neural circuitry, likely contribute to the therapeutic effects of hypothermia observed in ALS mouse models [75]. While such animal models provide valuable mechanistic information, it is well recognized that these interspecies distinctions limit the direct translation of findings to human neurobiology [75].

The customization of brain-guided programmed fever to enhance both efficacy and safety, nearly a century after Wagner-Jauregg's revolutionary, life-saving fever therapy, has been enabled by the discovery of the BTT, the first identified thermal waveguide in the human body, consisting of previously unrecognized bidirectional, bilateral pathways conducting thermal signals between the hypothalamus and the eyelid [46]. The discovery of the BTT has enabled, for the first time, noninvasive access to the hypothalamic thermoregulatory center, allowing continuous brain temperature monitoring via a noninvasive surface sensor placed on the eyelid, confirmed by recent studies showing brain cooling during yawning [47]. Studies have shown measurement of brain temperature noninvasively via the BTT during neurosurgery and distinguished BTT temperature measurements from those of neighboring skin as well as from blood surrounding the brain (e.g. during open-heart surgery) and ipsilateral to unilateral seizures [46]. Afferent thermal input from the eyelid skin to the brain is supported by the presence of heat-sensitive coatings on the trigeminal nerve as it courses along the wall of the cavernous sinus [76], at the terminal segment of the BTT [46].

Recognition of the BTT has enabled development of the computerized system presented herein, allowing precise modulation of both systemic and brain temperatures through cyclical increases and decreases in heat delivery to the body core via a thermal chamber and to the hypothalamic thermoregulatory center via a BTT thermal inductor positioned on the eyelid (Figure 1). Digital control of the thermal chamber and eyelid-mounted inductor allows CBIT^2 to maintain stable thermoregulation and brain-to-core temperature differentials that align with the body's natural fever threshold [10–18].

The sustained upregulation of HSPs and accompanying biomarker normalization support a disease-modifying effect; however, the durability of these benefits beyond the current 6-month follow-up remains unknown. Further studies and large clinical trials are required to determine whether repeated CBIT^2 sessions can achieve cure comparable to those historically observed with malarial fever therapy.

By brain-guided programmed fever offering a biologically supported method to augment endogenous HSP expression, it may enhance the effect of pharmacological chaperones like arimoclomol [68], supporting future studies on combining CBIT^2 with arimoclomol therapy addressing proteostasis restoration. Moreover, CBIT^2 through targeted induction of the heat shock response may provide a biologically complementary mechanism to existing FDA-approved ALS therapies and potentially enhance their therapeutic efficacy. Riluzole, which reduces glutamate-mediated excitotoxicity [22], may be potentiated by fever induced HSP-mediated neuroprotection via

 doi:10.20944/preprints202509.0342.v1

protein stabilization and attenuation of oxidative stress. Edaravone, an antioxidant that mitigates neuronal oxidative injury [60], may benefit from enhanced cellular resilience and free radical buffering induced by HSP-mediated programmed fever. For tofersen, an antisense oligonucleotide that reduces toxic SOD1 protein levels in ALS associated with SOD1 mutation [21], CBIT^2 may act synergistically by facilitating the refolding and clearance of misfolded proteins. This combination may support multimodal disease modification by addressing excitotoxicity, oxidative stress, and proteostasis dysfunction, complementing CBIT^2-induced heat shock protein activation as a unified strategy with pharmacological agents towards curing for ALS.

By activating HSPs and restoring proteostatic equilibrium, the brain-guided programmed thermofebrile activation introduced in this report offers a therapeutic strategy for reversing neurodegenerative pathology by directly targeting its root cause: misfolded proteins. What was once a mysterious clinical phenomenon that restored function and completely reversed disease in patients with dementia paralytica over 100 years ago is now revealed as a scientifically grounded molecular strategy targeting misfolded TDP-43, rekindling the long-dormant legacy of fever-based treatment, not as a historical curiosity, but as a renewed frontier in modern molecular medicine.

Beyond ALS, this breakthrough opens the path to treating and potentially curing other devastating neurodegenerative diseases, including Alzheimer's disease, Parkinson's disease, Huntington's disease, Lewy body dementia, the spinocerebellar ataxias, frontotemporal dementia, vascular dementia, multiple system atrophy, progressive supranuclear palsy, corticobasal degeneration, and prion diseases such as Creutzfeldt–Jakob disease, which are conditions long considered irreversible and uniformly fatal. In addition, the same mechanistic principles of protein misfolding reversal may extend to non-fatal but highly debilitating disorders such as autism spectrum disorders and diabetic neuropathy, widening the therapeutic horizon of brain-guided programmed fever.

This renewed molecular understanding of fever-induced therapeutic effects in neurological disease resulting in brain restoration, emerges at a critical moment in history. ALS, long regarded as irreversible and fatal, may now serve as a gateway for therapeutic innovation for effective neurological treatment amid one of the most urgent global health crises, as highlighted by the alarming announcement by the WHO that neurological disorders affect over 3 billion people worldwide [2]. Moreover, according to the WHO neurological disorders are the leading cause of disability [2], posing a profound threat to societal stability by diminishing workforce capacity, increasing long-term care demands, and straining healthcare systems worldwide. In the United States alone, Alzheimer's disease generated $360 billion in direct costs in 2024 [77], projected to reach $384 billion in 2025 [78], with an additional $413 billion linked to 19 billion hours of unpaid caregiving [78], totaling an annual burden of $773 billion, revealing a looming socioeconomic crisis worldwide. As WHO Director-General Dr. Tedros A. Ghebreyesus warned, *"Neurological conditions cause great suffering to the individuals and families, they rob communities and economies of human capital"*[2].

Neurological disorders now constitute one of the most debilitating and economically destabilizing health burdens worldwide, affecting cognition, motor control, speech, and even vital functions such as swallowing and respiration. A central driver of this crisis is the pathological accumulation of misfolded proteins across multiple age groups, disrupting brain function in conditions ranging from ALS in otherwise healthy individuals and elite athletes to Alzheimer's and Parkinson's disease in the aging population. The global wave of protein misfolding disorders extends even to the young as Autism Spectrum Disorder (ASD), is increasingly being recognized as involving disrupted proteostasis [79], which may be responsive to therapies that activate HSPs [80]. The well-documented 'fever effect', where febrile illness transiently improves behavioral symptoms in ASD, suggests that endogenous fever pathways can modulate neurological function [81]. This effect is further supported by studies demonstrating that sulforaphane improves ASD symptoms through activation of the heat shock response and upregulation of HSPs [80].

Proteopathic disorders are increasingly linked to this global public health emergency, as neurological diseases now affect more than one in three people worldwide. With the WHO projecting

 doi:10.20944/preprints202509.0342.v1

neurological disorders to become the second leading cause of death globally, today's crisis of disability is on track to become a mass mortality event [3]. This escalating threat compels a renewed scientific focus on therapeutic fever, first documented in a 1917 case report describing recovery from dementia paralytica [15]. Now, 108 years later, this ALS case report may serve as its modern molecularly based counterpart, reopening the possibility that advanced neurodegeneration can be therapeutically reversed. However, unlike the localized threat of neurosyphilis a century ago, today's challenge is global as misfolded proteins are now recognized as central drivers of the most prevalent and debilitating neurological disorders.

The successful induction of therapeutic fever using CBIT^2 in ALS, a disease historically regarded as uniformly progressive and notably resistant to treatment due to its exceptionally high threshold for HSP induction [24], reframes this terminal condition as a potential therapeutic gateway. In this case report, the comprehensive restoration of motor and cognitive function following CBIT^2 demonstrates that even the most treatment-refractory neuronal populations, such as motor neurons, can undergo recovery through the reactivation of endogenous repair mechanisms. If proteostatic resistance can be overcome in ALS, it is plausible that brain regions with lower activation thresholds may exhibit even greater response. Indeed, preliminary findings from ongoing applications of CBIT^2 in other misfolding-related disorders including Alzheimer's disease, Parkinson's disease, Huntington's disease, progressive supranuclear palsy, and ataxias have revealed clinical and biomarker changes suggestive of disease modification and brain restoration.

These therapeutic effects likely reflect the molecular reactivation of cytoprotective pathways, including HSP–mediated refolding of misfolded proteins such as TDP-43, restoration of proteostasis, and stabilization of neuronal structure and function. Together, these processes support the biological and molecular rationale for therapeutic fever as a strategy capable of restoring functional neural networks, opening new possibilities for care and redefining what is achievable in the treatment of neurodegenerative disease. Collectively, these results position ALS not only as a clinical inflection point but as a critical entry point to developing disease-modifying therapies, addressing its molecular roots, across diverse neurodegenerative as well as neurodevelopmental pathologies as ASD.

Patient perspective

Following CBIT^2, functional gains continue to advance and remained strikingly evident. At a local golf course, 3 months after CBIT^2 the patient walked unaided to the green with restored balance and motor control. She lined up her putt and sank the ball into the hole, twice in succession. Further underscoring her recovery, she later shared a video of herself putting at home, sending the ball into the cup with a single, fluid swing on her first attempt (Video S16) in addition to returning to play pickleball (Video S17). While visually impressive, these moments conveyed something beyond what any clinical scale, test, or biomarker could capture: the restoration of ordinary life, the freedom to live life to the fullest once more, echoing the profound and complete recoveries documented a century ago during malarial fever therapy. This regained ability to play golf and pickleball revealed a clinically meaningful restoration of neuromotor precision, postural control, balance, and complex coordination, capacities once considered irretrievable in the course of ALS.

5. Conclusions

This case report demonstrates, for the first time, that ALS, long regarded as an irreversible and uniformly fatal neurodegenerative disorder, can be reversed through CBIT^2, a fully noninvasive treatment that reengineers the 1927 Nobel Prize–recognized malarial fever therapy into a modern, intelligent, brain-guided digital intervention.

The patient, a 56-year-old woman, was diagnosed with ALS at the Mayo Clinic, based on electromyography confirming denervation and fasciculations along with neurological and MRI findings. Northwestern University independently confirmed the diagnosis and continued her on FDA-approved ALS drugs riluzole and edaravone. Despite expert management at both institutions, her disease progressed relentlessly, consistent with expectations for ALS, a disorder defined by paralysis, respiratory failure, and death.

 doi:10.20944/preprints202509.0342.v1

Yet following treatment by Dr. Marc Abreu in his private practice at the BTT Medical Institute, using CBIT² delivered through an FDA-approved computerized platform, this fatal trajectory was not merely slowed but fundamentally transformed achieving neurological, molecular, and electrophysiological reversal of ALS. Electromyography revealed the disappearance of denervation and fasciculations, signifying eradication of motor neuron death, while biomarkers shifted toward recovery with reductions in neurofilament light chain and homocysteine, normalization of IL-10 (with levels prior to CBIT² linked to increased mortality), and a dramatic rise in HSP70 expression. Correspondingly, the patient progressed from walker dependence to restored gait, safe swallowing, improved respiration, enhanced speech, and cognition restored to normal score. Most strikingly, she regained the ability to perform complex motor tasks including walking unaided onto a golf green, sinking consecutive putts, and playing pickleball, signaling not only survival, but a return to full life once thought irretrievably lost. Confronted with the extraordinary absence of diagnostic evidence for ALS, her Northwestern neurologist discontinued all ALS-specific medications, an outcome previously unimaginable for ALS.

Dr. Wagner-Jauregg's pioneering case report, published more than a century ago, described the reversal of dementia paralytica through deliberate fever induction [15], the first step in revealing fever's curative potential for neuropsychiatric disease. Initially met with skepticism, clinical trials confirmed its effects, reshaping neurology and psychiatry and earning recognition by the 1927 Nobel Prize. In that same lineage, the current report extends Wagner-Jauregg's vision into the modern era with digital precision. Using CBIT², fever is no longer a dangerous byproduct of infection but a brain-guided, programmable therapy delivered safely and noninvasively through the Brain–Eyelid Thermoregulatory Tunnel (BTT). Just as malarial fever once restored patients from the devastation of neurosyphilis, CBIT² here restored a patient from the devastation of ALS, a disease long considered irreversible and fatal.

This convergence of digital medicine and neurobiology reawakens the Nobel-recognized principle that fever can restore neurological function, offering a molecularly grounded strategy for disease reversal. Unlike externally applied heat or conventional hyperthermia, which often fail to trigger the heat shock response and may provoke physiological distress or even fatal complications, CBIT² operates in synchrony with hypothalamic thermoregulation, enabling safe, titrated, and effective induction of therapeutic fever with robust HSP activation. This fully noninvasive procedure exhibited an excellent safety profile, with no adverse events observed during treatment, within the critical 48-hour post-treatment window, or across six months of follow-up.

Beyond the confines of this case, our intervention responds to a broader global emergency, aligned with the Brain Economy Declaration at the June 2025 Brain Economy Summit, where G7 leaders urged prioritization of brain health as essential economic and societal infrastructure. In this context, the tragic irony of the Ice Bucket Challenge, co-founded by ALS patient Pete Frates, engaging over 440 million people and virtually every major celebrity and many heads of state, which raised hundreds of millions of dollars, yet yielding no therapeutic breakthrough while Frates himself died of ALS, which underscores the urgency of translating awareness into cures.

Taken together, these insights provide a compelling rationale for rigorous, large-scale clinical trials to confirm reproducibility, define durability, and establish the broader therapeutic potential of CBIT². What begins here with ALS may extend to Alzheimer's disease, Parkinson's disease, Huntington's disease, Lewy body dementia, spinocerebellar ataxias, frontotemporal dementia, multiple system atrophy, progressive supranuclear palsy, prion diseases, and beyond. The same molecular misfolding protein logic may also apply to nonfatal but debilitating disorders such as autism spectrum disorder and diabetic neuropathy.

By reviving Nobel Prize–recognized fever therapy a century later, not as memory but as method, CBIT² transforms medical history into medical future, opening a new frontier where brain function can be restored, lives reclaimed, and the trajectory of the global neurological crisis fundamentally changed. What is ultimately at stake is nothing less than the preservation of thought, memory, movement, and independence for over one third of humanity.

 doi:10.20944/preprints202509.0342.v1

Supplementary Materials: The following supporting information can be downloaded at the website of this paper posted on Preprints.org. Video S1: Left arm curls with 5-lb weights; Video S2: Right arm curls with 5-lb weights; Video S3: Sustained palmar holding of 1-lb weight (left side); Video S4: Sustained pinching holding of 2-lb weight (left side); Video S5: Sustained seated leg raise elevation (right side); Video S6: Sustained seated leg raise elevation (left side); Video S7: Ability to turn in bed (before treatment); Video S8: Gait measurement before treatment; Video S9: Gait measurement after treatment; Video S10: Lower extremity agility (cross-leg) before treatment; Video S11: Lower extremity agility (walk on toes) before treatment; Video S12: Lower extremity agility (dorsiflexion) after treatment; Video S13: IOPI anterior tongue endurance value before and after the first CBIT² session (close-up view); Video S14: IOPI posterior tongue endurance value before and after the first CBIT² session (close-up view); Video S15: IOPI lip strength evaluation (left side); Video S16: Demonstration of the patient's ability to play golf following CBIT² treatment; Video S17: Demonstration of the patient's ability to play pickleball following CBIT² treatment.

Author Contributions: Conceptualization, MMA and DGS; methodology, MMA; formal analysis, MMA, DGS, MHF; investigation, MMA, MHF; resources, MMA; data curation, MMA, DGS, MHF; writing—original draft preparation, MMA and DGS; writing—review and editing, MMA, DGS, MHF; visualization, MHF. All authors have read and agreed to the published version of the manuscript.

Funding: This case report was supported by the home institutions of the investigators. The technology applied to the treatment was supported in part by the Qualifying Therapeutic Discovery Project grant from the U.S. Federal Government.

Institutional Review Board Statement: Not applicable.

Informed Consent Statement: Written informed consent has been obtained from the patient to publish this paper.

Data Availability Statement: The original contributions presented in this study are included in the article/supplementary material. Further inquiries can be directed to the corresponding authors.

Acknowledgments: We thank Marcio de Jesus Dultra for design and drawing of schematics of BTT equipment.

Conflicts of Interest: MMA is a full-time employee at the BTT Medical Institute and holds patents with BTT Corp on engineering, software, and methods for BTT devices and sensors. MHF is a consultant for engineering and software for the BTT Medical Institute. The other author declare that he has no competing interests or personal relationships that could have appeared to influence the work reported in this article.

Dedication: This report is dedicated to the memory of Mike Borchetta, who tragically passed away from ALS just three days before his scheduled treatment at the BTT Medical Institute. His courage and hope remain an enduring inspiration, embodied by his determination to live, proven by his resolve, while already severely debilitated, to undertake the journey from Tennessee to Florida in pursuit of therapy. His passing has been a driving force behind the writing of this case report and underscores, with painful clarity, the urgency of advancing and expanding fever-based therapies. We hope that by disseminating this treatment and encouraging its adoption by other physicians, future patients may live to benefit in time. Mike's determination continues to guide this work as we strive to turn possibility into reality for those facing ALS and related neurodegenerative diseases.

Abbreviations

The following abbreviations are used in this manuscript:

ALS	Amyotrophic Lateral Sclerosis
ALSFRS	Amyotrophic Lateral Sclerosis Functional Rating Scale
ASD	Autism Spectrum Disorder
BTT	Brain-Eyelid Thermoregulatory Tunnel
CBIT²	Computerized Brain-Guided Intelligent Thermofebrile Therapy
CK	Creatine Kinase
COP	Center of pressure

 doi:10.20944/preprints202509.0342.v1

EMG	Electromyography
FAEO	Feet apart and eyes open
FDA	Food and Drug Administration
FEV1	Forced Expiratory Volume in 1 second
FLAIR	Fluid-attenuated inversion recovery
FTEC	Feet together with eyes closed
FTEO	Feet together with eyes open
FVC	Forced vital capacity
HSP	Heat shock protein
IL-10	Interleukin-10
IOPI	Iowa Oral Performance Instrument
IVIg	Intravenous immunoglobulin
JNK	c-Jun N-terminal Kinase
MoCA	Montreal Cognitive Assessment
MRI	Magnetic Resonance Imaging
NF-κB	Nuclear factor kappa B
NfL	Neurofilament light chain
SLR	Straight leg raise
SOD1	Superoxide dismutase-1
SWI	Susceptibility-weighted Imaging
TSH	Thyroid-stimulating Hormone
TUG	Timed Up and Go
WHO	World Health Organization

Appendix A

Appendix A.1

Appendix A1 presents the EMG report performed on 25 October 2024, at Mayo Clinic Rochester.

Appendix A.2

Appendix A2 presents the EMG report performed on 24 June 2025, at Northwestern Medicine, 5 months after the first treatment.

Appendix B

Appendix B presents the report of hearing assessment using automated auditory sensitivity testing (GSI AMTAS) conducted before and after CBIT² treatment.

References

1. Canada Brain Research Strategy. Canada Brain Economy Declaration. Available online: https://canadianbrain.ca/canada-brain-economy-declaration/ (accessed Aug 19, 2025).
2. World Health Organization. Over 1 in 3 people affected by neurological conditions, the leading cause of illness and disability worldwide. Available online: https://www.who.int/news/item/14-03-2024-over-1-in-3-people-affected-by-neurological-conditions--the-leading-cause-of-illness-and-disability-worldwide (accessed Aug 5, 2025).
3. World Health Organization. Launch of first WHO position paper on optimizing brain health across life. Available online: https://www.who.int/news/item/09-08-2022-launch-of-first-who-position-paper-on-optimizing-brain-health-across-life (accessed Aug 19, 2025).
4. Feldman, E. L.; Goutman, S. A.; Petri, S.; Mazzini, L.; Savelieff, M. G.; Shaw, P. J.; Sobue, G. Amyotrophic Lateral Sclerosis. *Lancet* **2022**, *400* (10360), 1363–1380. https://doi.org/10.1016/S0140-6736(22)01272-7.
5. Brown, R. H.; Al-Chalabi, A. Amyotrophic Lateral Sclerosis. *N Engl J Med* **2017**, *377* (2), 162–172. https://doi.org/10.1056/NEJMRA1603471.

 doi:10.20944/preprints202509.0342.v1

6. Crockford, C.; Newton, J.; Lonergan, K.; Chiwera, T.; Booth, T.; Chandran, S.; Colville, S.; Heverin, M.; Mays, I.; Pal, S.; et al. ALS-Specific Cognitive and Behavior Changes Associated with Advancing Disease Stage in ALS. *Neurology* **2018**, *91* (15), E1370–E1380. https://doi.org/10.1212/WNL.0000000000006317.
7. Ringholz, G. M.; Appel, S. H.; Bradshaw, M.; Cooke, N. A.; Mosnik, D. M.; Schulz, P. E. Prevalence and Patterns of Cognitive Impairment in Sporadic ALS. *Neurology* **2005**, *65* (4), 586–590. https://doi.org/10.1212/01.WNL.0000172911.39167.B6.
8. Lewis, M.; Gordon, P. H. Lou Gehrig, Rawhide, and 1938. *Neurology* **2007**, *68* (8), 615–618. https://doi.org/10.1212/01.WNL.0000254623.04219.AA.
9. Brennan, F. The 70th Anniversary of the Death of Lou Gehrig. *Am J Hosp Palliat Care* **2012,** *29* (7), 512–514. https://doi.org/10.1177/1049909111434635.
10. The Nobel Prize. Julius Wagner-Jauregg – Nobel Lecture. Available online: https://www.nobelprize.org/prizes/medicine/1927/wagner-jauregg/lecture/ (accessed Aug 7, 2025).
11. Tsay, C. J. Julius Wagner-Jauregg and the Legacy of Malarial Therapy for the Treatment of General Paresis of the Insane. *Yale J Biol Med* **2013,** *86* (2), 245. https://pmc.ncbi.nlm.nih.gov/articles/PMC3670443/.
12. Whitrow, M. Wagner-Jauregg and Fever Therapy. *Med Hist* **1990**, *34* (3), 294–310. https://doi.org/10.1017/S0025727300052431.
13. Wagner-Jauregg, J.; Bruetsch, W. L. The History of the Malaria Treatment of General Paralysis. *Am J Psychiatry* **1946**, *102*, 577–582. https://doi.org/10.1176/AJP.102.5.577.
14. Daey Ouwens, I. M.; Lens, C. E.; Fiolet, A. T. L.; Ott, A.; Koehler, P. J.; Kager, P. A.; Verhoeven, W. M. A. Malaria Fever Therapy for General Paralysis of the Insane: A Historical Cohort Study. *Eur Neurol* **2017**, *78* (1–2), 56–62. https://doi.org/10.1159/000477900.
15. Wagner-Jauregg, J. Über Die Einwirkung Der Malaria Auf Die Progressive Paralyse. [On the Effect of Malaria on Progressive Paralysis], *Psychiat neurol Wochenschrift* **1918-1919**, 20 (132–134).
16. Wagner-Jauregg, J. Verhütung Und Behandlung Der Progressiven Paralyse Durch Impfmalaria [Prevention and Treatment of Progressive Paralysis by Malaria Inoculation], Handbuch der experimentellen Therapie Ergänzungsband: Munich, **1931**.
17. Zuschlag, Z. D.; Lalich, C. J.; Short, E. B.; Hamner, M.; Kahn, D. A. Pyrotherapy for the Treatment of Psychosis in the 21st Century: A Case Report and Literature Review. *J Psychiatr Pract* **2016,** *22* (5), 410–415. https://doi.org/10.1097/PRA.0000000000000181.
18. Karamanou, M.; Liappas, I.; Antoniou, C.; Androutsos, G.; Lykouras, E. Julius Wagner-Jauregg (1857-1940): Introducing Fever Therapy in the Treatment of Neurosyphilis. *Psychiatriki* **2013,** *24* (3), 208–212.
19. Stereowise Plus. ASUS & Brain Tunnelgenix Technologies partner to deliver first PC-Based, FDA-Approved temperature monitoring system. Available online: https://www.stereowiseplus.com/2010/10/asus-brain-tunnelgenix-technologies.html (accessed Aug 19, 2025).
20. Benatar, M.; Hansen, T.; Rom, D.; Geist, M. A.; Blaettler, T.; Camu, W.; Kuzma-Kozakiewicz, M.; van den Berg, L. H.; Morales, R. J.; Chio, A.; et al. Safety and Efficacy of Arimoclomol in Patients with Early Amyotrophic Lateral Sclerosis (ORARIALS-01): A Randomised, Double-Blind, Placebo-Controlled, Multicentre, Phase 3 Trial. *Lancet Neurol* **2024**, *23* (7), 687–699. https://doi.org/10.1016/S1474-4422(24)00134-0.
21. Hamad, A. A.; Alkhawaldeh, I. M.; Nashwan, A. J.; Meshref, M.; Imam, Y. Tofersen for SOD1 Amyotrophic Lateral Sclerosis: A Systematic Review and Meta-Analysis. *Neurol Sci* **2025**, *46* (5), 1977–1985. https://doi.org/10.1007/S10072-025-07994-2.
22. Bensimon, G.; Lacomblez, L.; Meininger, V. A Controlled Trial of Riluzole in Amyotrophic Lateral Sclerosis. ALS/Riluzole Study Group. *N Engl J Med*, **1994**, *330* (9), 585–591. https://doi.org/10.1056/NEJM199403033300901.
23. Miller, R. G.; Mitchell, J. D.; Moore, D. H. Riluzole for Amyotrophic Lateral Sclerosis (ALS)/Motor Neuron Disease (MND). *Cochrane Database Syst Rev* **2012**, *2012* (3). https://doi.org/10.1002/14651858.CD001447.PUB3.
24. Batulan, Z.; Shinder, G. A.; Minotti, S.; He, B. P.; Doroudchi, M. M.; Nalbantoglu, J.; Strong, M. J.; Durham, H. D. High Threshold for Induction of the Stress Response in Motor Neurons Is Associated with Failure to Activate HSF1. *J Neurosci* **2003**, *23* (13), 5789–5798. https://doi.org/10.1523/JNEUROSCI.23-13-05789.2003.

 doi:10.20944/preprints202509.0342.v1

25. Storkebaum, E.; Rosenblum, K.; Sonenberg, N. Messenger RNA Translation Defects in Neurodegenerative Diseases. *N Eng J Med* **2023**, *388* (11), 1015–1030. https://doi.org/10.1056/NEJMRA2215795.
26. Smadja, D. M.; Abreu, M. M. Hyperthermia and Targeting Heat Shock Proteins: Innovative Approaches for Neurodegenerative Disorders and Long COVID. *Front Neurosci* **2025**, *19*. https://doi.org/10.3389/FNINS.2025.1475376.
27. Batulan, Z.; Taylor, D. M.; Aarons, R. J.; Minotti, S.; Doroudchi, M. M.; Nalbantoglu, J.; Durham, H. D. Induction of Multiple Heat Shock Proteins and Neuroprotection in a Primary Culture Model of Familial Amyotrophic Lateral Sclerosis. *Neurobiol Dis* **2006**, *24* (2), 213–225. https://doi.org/10.1016/J.NBD.2006.06.017.
28. Kalmar, B.; Greensmith, L. Cellular Chaperones as Therapeutic Targets in ALS to Restore Protein Homeostasis and Improve Cellular Function. *Front Mol Neurosci* **2017**, *10*. https://doi.org/10.3389/FNMOL.2017.00251.
29. Lackie, R. E.; Maciejewski, A.; Ostapchenko, V. G.; Marques-Lopes, J.; Choy, W. Y.; Duennwald, M. L.; Prado, V. F.; Prado, M. A. M. The Hsp70/Hsp90 Chaperone Machinery in Neurodegenerative Diseases. *Front Neurosci* **2017**, *11* (MAY). https://doi.org/10.3389/FNINS.2017.00254.
30. Brown, I. R. Heat Shock Proteins and Protection of the Nervous System. *Ann N Y Acad Sci* **2007**, *1113*, 147–158. https://doi.org/10.1196/ANNALS.1391.032.
31. Tedesco, B.; Ferrari, V.; Cozzi, M.; Chierichetti, M.; Casarotto, E.; Pramaggiore, P.; Mina, F.; Galbiati, M.; Rusmini, P.; Crippa, V.; et al. The Role of Small Heat Shock Proteins in Protein Misfolding Associated Motoneuron Diseases. *Int J Mol Sci* **2022**, *23* (19). https://doi.org/10.3390/IJMS231911759.
32. Gifondorwa, D. J.; Robinson, M. B.; Hayes, C. D.; Taylor, A. R.; Prevette, D. M.; Oppenheim, R. W.; Caress, J.; Milligan, C. E. Exogenous Delivery of Heat Shock Protein 70 Increases Lifespan in a Mouse Model of Amyotrophic Lateral Sclerosis. *J Neurosci* **2007**, *27* (48), 13173–13180. https://doi.org/10.1523/JNEUROSCI.4057-07.2007.
33. Garcia-Toscano, L.; Currey, H. N.; Hincks, J. C.; Stair, J. G.; Lehrbach, N. J.; Liachko, N. F. Decreased Hsp90 Activity Protects against TDP-43 Neurotoxicity in a C. Elegans Model of Amyotrophic Lateral Sclerosis. *PLoS Genet* **2024**, *20* (12). https://doi.org/10.1371/JOURNAL.PGEN.1011518.
34. Sharp, P.; Krishnan, M.; Pullar, O.; Navarrete, R.; Wells, D.; de Belleroche, J. Heat Shock Protein 27 Rescues Motor Neurons Following Nerve Injury and Preserves Muscle Function. *Exp Neurol* **2006**, *198* (2), 511–518. https://doi.org/10.1016/J.EXPNEUROL.2005.12.031.
35. Carman, A.; Kishinevsky, S.; Koren, J.; Lou, W.; Chiosis, G. Chaperone-Dependent Neurodegeneration: A Molecular Perspective on Therapeutic Intervention. *J Alzheimers Dis Parkinsonism* **2013**, *2013* (Suppl 10). https://doi.org/10.4172/2161-0460.S10-007.
36. Webster, C. P.; Smith, E. F.; Shaw, P. J.; De Vos, K. J. Protein Homeostasis in Amyotrophic Lateral Sclerosis: Therapeutic Opportunities? *Front Mol Neurosci* **2017**, *10*. https://doi.org/10.3389/FNMOL.2017.00123.
37. Kalmar, B.; Lu, C. H.; Greensmith, L. The Role of Heat Shock Proteins in Amyotrophic Lateral Sclerosis: The Therapeutic Potential of Arimoclomol. *Pharmacol Ther* **2014**, *141* (1), 40–54. https://doi.org/10.1016/J.PHARMTHERA.2013.08.003.
38. Schapira, A. H. V.; Olanow, C. W.; Greenamyre, J. T.; Bezard, E. Slowing of Neurodegeneration in Parkinson's Disease and Huntington's Disease: Future Therapeutic Perspectives. *The Lancet* **2014**, *384* (9942), 545–555. https://doi.org/10.1016/S0140-6736(14)61010-2.
39. Ciechanover, A.; Kwon, Y. T. Protein Quality Control by Molecular Chaperones in Neurodegeneration. *Front Neurosci* **2017**, *11* (APR). https://doi.org/10.3389/FNINS.2017.00185.
40. Noori, L.; Saqagandomabadi, V.; Di Felice, V.; David, S.; Caruso Bavisotto, C.; Bucchieri, F.; Cappello, F.; Conway de Macario, E.; Macario, A. J. L.; Scalia, F. Putative Roles and Therapeutic Potential of the Chaperone System in Amyotrophic Lateral Sclerosis and Multiple Sclerosis. *Cells 2024* **2024**, *13* (3), 217. https://doi.org/10.3390/CELLS13030217.
41. Hunt, A. P.; Minett, G. M.; Gibson, O. R.; Kerr, G. K.; Stewart, I. B. Could Heat Therapy Be an Effective Treatment for Alzheimer's and Parkinson's Diseases? A Narrative Review. *Front Physiol* **2020**, *10*, 1556. https://doi.org/10.3389/FPHYS.2019.01556.

 doi:10.20944/preprints202509.0342.v1

42. Sharma, R.; Khan, Z.; Mehan, S.; Das Gupta, G.; Narula, A. S. Unraveling the Multifaceted Insights into Amyotrophic Lateral Sclerosis: Genetic Underpinnings, Pathogenesis, and Therapeutic Horizons. *Mutat Res Rev Mutat Res* **2024**, *794*. https://doi.org/10.1016/J.MRREV.2024.108518.
43. Fadel, A.; Hussain, H.; Hernandez, R. J.; Clichy Silva, A. M.; Estil-las, A. A.; Hamad, M.; Saadoon, Z. F.; Naseer, L.; Sultan, W. C.; Sultan, C.; et al. Mechanisms of Neurosyphilis-Induced Dementia: Insights into Pathophysiology. *Neurol Int* **2024**, *16* (6), 1653–1665. https://doi.org/10.3390/NEUROLINT16060120.
44. Peart, K. Yale Researcher Discovers "Brain Temperature Tunnel" That For The First Time Allows External Continuous Measurement of Brain Temperature | Yale News. Available online: https://news.yale.edu/2003/07/02/yale-researcher-discovers-brain-temperature-tunnel-first-time-allows-external-continuou-0 (accessed Aug 5, 2025).
45. Abreu, M. M. US Patent; Identification and Characterization of the Brain Thermal Tunnel, February 26, **2003**. https://patents.google.com/patent/WO2005015163A2/no.
46. Abreu, M. M.; Smith, R. L.; Banack, T. M.; Arroyo, A. C.; Gochman, R. F.; Clebone, A. L.; Dai, F.; Bergeron, M. F.; Haddadin, A. S.; Silverman, T. J.; et al. Brain Thermal Kinetics at Brain-Eyelid Thermal Tunnels Overcoming COVID-19 Thermometry Limitations for Automated Asymptomatic Infection Detection in Concert with Physical and Biological Principles. *Authorea Preprints* **2021**. https://doi.org/10.22541/AU.163432121.14501499/V2.
47. Ramirez, V.; Ryan, C. P.; Eldakar, O. T.; Gallup, A. C. Manipulating Neck Temperature Alters Contagious Yawning in Humans. *Physiol Behav* **2019**, *207*, 86–89. https://doi.org/10.1016/J.PHYSBEH.2019.04.016.
48. Tayeb, Z.; Dragomir, A.; Lee, J. H.; Abbasi, N. I.; Dean, E.; Bandla, A.; Bose, R.; Sundar, R.; Bezerianos, A.; Thakor, N. V.; et al. Distinct Spatio-Temporal and Spectral Brain Patterns for Different Thermal Stimuli Perception. *Sci Rep* **2022**, *12* (1), 1–16. https://doi.org/10.1038/s41598-022-04831-w.
49. Scripture, E. W. The Need of Psychological Training. *Science (1979)* **1892**, *19* (474), 127–128. https://doi.org/10.1126/science.ns-19.474.127.
50. Newsweek. America's Best Neurological Hospitals 2024. Available online: https://rankings.newsweek.com/americas-best-neurological-hospitals-2024 (accessed Aug 28, 2025).
51. Hammerschmidt, S.; Wahn, H.; Langmann, P.; Scheppach, W. [Acute Liver Failure after Therapeutic Hyperthermia]. *Deutsche medizinische Wochenschrift* **1999**, *124* (46), 1379–1382. https://doi.org/10.1055/S-2007-1024543.
52. Abreu, M. M. New Concepts in Perioperative Normothermia: From Monitoring to Management. *Anesthesiology News* **2011**, 39–48. https://files.sld.cu/anestesiologia/files/2012/05/tempmanagement_anse11_wm2.pdf.
53. Kawamura, H.; Sawyer, C. H. Elevation in Brain Temperature during Paradoxical Sleep. *Science (1979)* **1965**, *150* (3698), 912–913. https://doi.org/10.1126/SCIENCE.150.3698.912.
54. Maloney, S. K.; Fuller, A.; Mitchell, G.; Mitchell, D. Rectal Temperature Measurement Results in Artifactual Evidence of Selective Brain Cooling. *Am J Physiol Regul Integr Comp Physiol* **2001**, *281* (1 50-1), 108–114. https://doi.org/10.1152/AJPREGU.2001.281.1.R108.
55. Rampone, A. J.; Shirasu, M. E. Temperature Changes in the Rat in Response to Feeding. *Science (1979)* **1964**, *144* (3616), 317–319. https://doi.org/10.1126/SCIENCE.144.3616.317.
56. Yang, X. F.; Chang, J. H.; Rothman, S. M. Intracerebral Temperature Alterations Associated with Focal Seizures. *Epilepsy Res* **2002**, *52* (2), 97–105. https://doi.org/10.1016/S0920-1211(02)00193-6.
57. Wu, T. W.; McLean, C.; Friedlich, P.; Wisnowski, J.; Grimm, J.; Panigrahy, A.; Bluml, S.; Seri, I. Brain Temperature in Neonates with Hypoxic-Ischemic Encephalopathy during Therapeutic Hypothermia. *J Pediatr* **2014**, *165* (6), 1129–1134. https://doi.org/10.1016/J.JPEDS.2014.07.022.
58. Castrillo-Viguera, C.; Grasso, D. L.; Simpson, E.; Shefner, J.; Cudkowicz, M. E. Clinical Significance in the Change of Decline in ALSFRS-R. *Amyotroph Lateral Scler* **2010**, *11* (1–2), 178–180. https://doi.org/10.3109/17482960903093710.
59. Abe, K.; Itoyama, Y.; Sobue, G.; Tsuji, S.; Aoki, M.; Doyu, M.; Hamada, C.; Kondo, K.; Yoneoka, T.; Akimoto, M.; et al. Confirmatory Double-Blind, Parallel-Group, Placebo-Controlled Study of Efficacy and Safety of Edaravone (MCI-186) in Amyotrophic Lateral Sclerosis Patients. *Amyotroph Lateral Scler Frontotemporal Degener* **2014**, *15* (7–8), 610. https://doi.org/10.3109/21678421.2014.959024.

60. Writing Group; Edaravone (MCI-186) ALS 19 Study Group; Abe, K.; Aoki, M.; Tsuji, S.; Itoyama, Y.; Sobue, G.; Togo, M.; Hamada, C.; Tanaka, M.; et al. Safety and Efficacy of Edaravone in Well Defined Patients with Amyotrophic Lateral Sclerosis: A Randomised, Double-Blind, Placebo-Controlled Trial. *Lancet Neurol* **2017**, *16* (7), 505–512. https://doi.org/10.1016/S1474-4422(17)30115-1.
61. Benatar, M.; Macklin, E. A.; Malaspina, A.; Rogers, M. L.; Hornstein, E.; Lombardi, V.; Renfrey, D.; Shepheard, S.; Magen, I.; Cohen, Y.; et al. Prognostic Clinical and Biological Markers for Amyotrophic Lateral Sclerosis Disease Progression: Validation and Implications for Clinical Trial Design and Analysis. *EBioMedicine* **2024**, *108*, 105323. https://doi.org/10.1016/J.EBIOM.2024.105323.
62. Olesen, M. N.; Wuolikainen, A.; Nilsson, A. C.; Wirenfeldt, M.; Forsberg, K.; Madsen, J. S.; Lillevang, S. T.; Brandslund, I.; Andersen, P. M.; Asgari, N. Inflammatory Profiles Relate to Survival in Subtypes of Amyotrophic Lateral Sclerosis. *Neurol Neuroimmunol Neuroinflamm* **2020**, *7* (3). https://doi.org/10.1212/NXI.0000000000000697.
63. Zoccolella, S.; Simone, I. L.; Lamberti, P.; Samarelli, V.; Tortelli, R.; Serlenga, L.; Logroscino, G. Elevated Plasma Homocysteine Levels in Patients with Amyotrophic Lateral Sclerosis. *Neurology* **2008**, *70* (3), 222–225. https://doi.org/10.1212/01.WNL.0000297193.53986.6F.
64. Chen, S.; Brown, I. R. Neuronal Expression of Constitutive Heat Shock Proteins: Implications for Neurodegenerative Diseases. *Cell Stress Chaperones* **2007**, *12* (1), 51–58. https://doi.org/doi:10.1379/csc-236r.1.
65. San Gil, R.; Ooi, L.; Yerbury, J. J.; Ecroyd, H. The Heat Shock Response in Neurons and Astroglia and Its Role in Neurodegenerative Diseases. *Mol Neurodegener* **2017**, *12* (1), 1–20. https://doi.org/10.1186/S13024-017-0208-6.
66. Dukay, B.; Csoboz, B.; Tóth, M. E. Heat-Shock Proteins in Neuroinflammation. *Front Pharmacol* **2019**, *10* (JULY). https://doi.org/10.3389/FPHAR.2019.00920.
67. Garbuz, D. G.; Zatsepina, O. G.; Evgen'ev, M. B. Beta Amyloid, Tau Protein, and Neuroinflammation: An Attempt to Integrate Different Hypotheses of Alzheimer's Disease Pathogenesis. *Mol Biol* **2021**, *55* (5), 670–682. https://doi.org/10.1134/S002689332104004X.
68. Kuta, R.; Larochelle, N.; Fernandez, M.; Pal, A.; Minotti, S.; Tibshirani, M.; St. Louis, K.; Gentil, B. J.; Nalbantoglu, J. N.; Hermann, A.; et al. Depending on the Stress, Histone Deacetylase Inhibitors Act as Heat Shock Protein Co-Inducers in Motor Neurons and Potentiate Arimoclomol, Exerting Neuroprotection through Multiple Mechanisms in ALS Models. *Cell Stress Chaperones* **2020**, *25* (1), 173–191. https://doi.org/10.1007/S12192-019-01064-1.
69. Clarke, B. E.; Gil, R. S.; Yip, J.; Kalmar, B.; Greensmith, L. Regional Differences in the Inflammatory and Heat Shock Response in Glia: Implications for ALS. *Cell Stress Chaperones* **2019**, *24* (5), 857. https://doi.org/10.1007/S12192-019-01005-Y.
70. Yu, W. W.; Cao, S. N.; Zang, C. X.; Wang, L.; Yang, H. Y.; Bao, X. Q.; Zhang, D. Heat Shock Protein 70 Suppresses Neuroinflammation Induced by α-Synuclein in Astrocytes. *Mol Cel Neurosci* **2018**, *86*, 58–64. https://doi.org/10.1016/J.MCN.2017.11.013.
71. Borges, T. J.; Lopes, R. L.; Pinho, N. G.; Machado, F. D.; Souza, A. P. D.; Bonorino, C. Extracellular Hsp70 Inhibits Pro-Inflammatory Cytokine Production by IL-10 Driven down-Regulation of C/EBPβ and C/EBPδ. *Int J Hyperthermia* **2013**, *29* (5), 455–463. https://doi.org/10.3109/02656736.2013.798037.
72. Doeppner, T. R.; Kaltwasser, B.; Fengyan, J.; Hermann, D. M.; Bähr, M. TAT-Hsp70 Induces Neuroprotection against Stroke via Anti-Inflammatory Actions Providing Appropriate Cellular Microenvironment for Transplantation of Neural Precursor Cells. *J Cereb Blood Flow Meta* **2013**, *33* (11), 1778. https://doi.org/10.1038/JCBFM.2013.126.
73. Smadja, D. M. Hyperthermia for Targeting Cancer and Cancer Stem Cells: Insights from Novel Cellular and Clinical Approaches. *Stem Cell Rev Rep* **2024**, *20* (6), 1532–1539. https://doi.org/10.1007/S12015-024-10736-0.
74. Martin, L. J.; Niedzwiecki, M. V.; Wong, M. Chronic Intermittent Mild Whole-Body Hypothermia Is Therapeutic in a Mouse Model of ALS. *Cells* **2021**, *10* (2), 320. https://doi.org/10.3390/CELLS10020320.

75. Hodge, R. D.; Bakken, T. E.; Miller, J. A.; Smith, K. A.; Barkan, E. R.; Graybuck, L. T.; Close, J. L.; Long, B.; Johansen, N.; Penn, O.; et al. Conserved Cell Types with Divergent Features in Human versus Mouse Cortex. *Nature* **2019**, *573* (7772), 61–68. https://doi.org/10.1038/s41586-019-1506-7.
76. Liu, L.; Simon, S. A. Capsaicin, Acid and Heat-Evoked Currents in Rat Trigeminal Ganglion Neurons: Relationship to Functional VR1 Receptors. *Physiol Behav* **2000**, *69* (3), 363–378. https://doi.org/10.1016/S0031-9384(00)00209-2.
77. 2024 Alzheimer's Disease Facts and Figures. *Alzheimers Dement* **2024**, *20* (5), 3708–3821. https://doi.org/10.1002/ALZ.13809.
78. Alzheimer's Association. Alzheimer's Facts and Figures Report. Available online: https://www.alz.org/alzheimers-dementia/facts-figures (accessed Aug 19, 2025).
79. Singh, K.; Connors, S. L.; Macklin, E. A.; Smith, K. D.; Fahey, J. W.; Talalay, P.; Zimmerman, A. W. Sulforaphane Treatment of Autism Spectrum Disorder (ASD). *Proc Natl Acad Sci U S A* **2014**, *111* (43), 15550–15555. https://doi.org/10.1073/PNAS.1416940111.
80. Gan, N.; Wu, Y. C.; Brunet, M.; Garrido, C.; Chung, F. L.; Dai, C.; Mi, L. Sulforaphane Activates Heat Shock Response and Enhances Proteasome Activity through Up-Regulation of Hsp27. *J Biol Chem* **2010**, *285* (46), 35528–35536. https://doi.org/10.1074/JBC.M110.152686.
81. Zimmerman, A.; Diggins, E.; Connors, S.; Singh, K. Sulforaphane Treatment of Children with Autism Spectrum Disorder (ASD) – A Progress Report (N1.002). *Neurology* **2018**, *90* (15_supplement), N1.002. https://doi.org/10.1212/WNL.90.15_SUPPLEMENT.N1.002.